FOR OFFICIAL USE ONLY

JPRS L/8341

16 March 1979

[redacted]

USSR

[redacted]

[redacted]

TRANSLATIONS ON USSR SCIENCE AND TECHNOLOGY
PHYSICAL SCIENCES AND TECHNOLOGY
(FOUO 16/79)

U. S. JOINT PUBLICATIONS RESEARCH SERVICE

[redacted]

FOR OFFICIAL USE ONLY

APPROVED FOR RELEASE: 2007/02/08: CIA-RDP82-00850R000100030044-9

NOTE

JPRS publications contain information primarily from foreign newspapers, periodicals and books, but also from news agency transmissions and broadcasts. Materials from foreign-language sources are translated; those from English-language sources are transcribed or reprinted, with the original phrasing and other characteristics retained.

Headlines, editorial reports, and material enclosed in brackets [] are supplied by JPRS. Processing indicators such as [Text] or [Excerpt] in the first line of each item, or following the last line of a brief, indicate how the original information was processed. Where no processing indicator is given, the information was summarized or extracted.

Unfamiliar names rendered phonetically or transliterated are enclosed in parentheses. Words or names preceded by a question mark and enclosed in parentheses were not clear in the original but have been supplied as appropriate in context. Other unattributed parenthetical notes within the body of an item originate with the source. Times within items are as given by source.

The contents of this publication in no way represent the policies, views or attitudes of the U.S. Government.

APPROVED FOR RELEASE: 2007/02/08: CIA-RDP82-00850R000100030044-9

BIBLIOGRAPHIC DATA SHEET	1. Report No. JPRS L/8341	2.	3. Recipient's Accession No.
4. Title and Subtitle TRANSLATIONS ON USSR SCIENCE AND TECHNOLOGY - PHYSICAL SCIENCES AND TECHNOLOGY, (FOUO 16/79)			5. Report Date 16 March 1979 6.
7. Author(s)			8. Performing Organization Rept. No.
9. Performing Organization Name and Address Joint Publications Research Service 1000 North Glebe Road Arlington, Virginia 22201			10. Project/Task/Work Unit No. 11. Contract/Grant No.
12. Sponsoring Organization Name and Address As above			13. Type of Report & Period Covered 14.

15. Supplementary Notes

16. Abstract

The report contains information on aeronautics; astronomy and astrophysics; atmospheric sciences; chemistry; earth sciences and oceanography; electronics and electrical engineering; energy conversion; materials; mathematical sciences; cybernetics, computers; mechanical, industrial, civil, and marine engineering; methods and equipment; missile technology; navigation, communications, detection, and countermeasures, nuclear science and technology; ordnance; physics; propulsion and fuels; space technology; and scientists and scientific organization in the physical sciences.

17. Key Words and Document Analysis. 17a. Descriptors

USSR
Aeronautics
Astronomy
Astrophysics
Atmospheric Sciences
Chemistry
Computers
Cybernetics
Earth Sciences
Oceanography
Electronics
Electrical Engineering
Energy Conversion
Materials
Mathematics
Mechanical Engineering
Civil Engineering
Industrial Engineering
Marine Engineering
Methods
Equipment
Missile Technology
Navigation and Communications
Detection and Countermeasures
Nuclear Science and Technology
Ordnance
Physics
Propulsion and Fuels
Space Technology

17b. Identifiers/Open-Ended Terms

17c. COSATI Field/Group 01,03,04,07,08,09,10,11,12,13,14,16,17,18,19,20,21,22

18. Availability Statement	19. Security Class (This Report)	21. No. of Pages
For Official Use Only. Limited Number of Copies Available From JPRS	UNCLASSIFIED	81
	20. Security Class (This Page) UNCLASSIFIED	22. Price

FORM NTIS-35 (10-70)

THIS FORM MAY BE REPRODUCED

USCOMM-DC 14952-P72

JPRS L/8341

16 March 1979

TRANSLATIONS ON USSR SCIENCE AND TECHNOLOGY
PHYSICAL SCIENCES AND TECHNOLOGY

(FOUO 16/79)

CONTENTS

CONTENTS (Continued) Page

ELECTRONICS AND ELECTRICAL ENGINEERING

UDC 621.391.161

SPATIAL-TIME PROCESSING OF RADIO SIGNALS IN RADIO MEASUREMENT SYSTEMS IN THE GENERAL CASE (REVIEW)

Kiev IVUZ RADIOELEKTRONIKA in Russian Vol 21 No 11, Nov 78 pp 3-15

[Article by I.Ya. Kremer and G.S. Nakhmanson, manuscript received following revision 10 May, 1978]

[Text] Optimal spatial-time processing of signals is considered in the general case, including the location of the objects and external interference sources being observed in both the far field of the receiving antenna systems as well as in the Fresnel zone. Also analyzed are the possibilities of utilyzing information on the curvature of the wave front of signals and interference to increase the precision in the determination of the location of the observed objects, increase the resolving power of the system and discriminates signals from interference generated by external sources.

Introduction

The basic principles of the theory of optimal spatial-time processing of signals in determining the position of observed objects and the parameters of their motion have been rather thoroughly worked out in the literature [1 - 3], etc. However, specific results in this field have been primarily obtained as applied to the special case where the wave fronts of the signals in the external interference can be considered planar, i.e., the observed objects and interference sources are located in the far field of the receiving antenna systems, something which is justified only when the following condition is met:

$$R \leqslant R_{дз} = \frac{2L^2 \cos\theta}{\lambda}, \qquad (1)$$

where R is the distance of the radiation source from the center of the antenna; $R_{дз}$ is the radius of the far field; L is the overall dimension of the receiving antenna system; θ is the angle between the normal to the plane of the antenna and direction to the source; λ is the wavelength.

The effort to increase the resolving power of radio measurement systems and, related to this, the trend towards the use of large antenna systems and the mastery of increasingly shorter wavelengths, as well as the use of diversity receiving systems [4, 5] is leading to the fact in a number of cases, condition (1) is not met and it is impossible to consider the wave fronts of the signals being processed to be planar ones. T us, the basic relationships derived for the case of plane electromagnetic waves are not applicable to the analysis and synthesis of optimal spatial-time signal processing algorithms in a number of radio measurement systems and the theory of several such systems (multiposition radar systems [5], hyperbolic radio navigation systems [6], etc.) are at times developed independently of the general theory of spatial-time processing signals. This makes the analysis of such signals difficult based on uniform methodological principles of optimal reception theory, as well as the estimation of the closeness of their characteristics to the potential achievable ones and the determination of ways of optimizing them. What has been said above can also apply to sonar systems. For this reason, an urgent problem is the generalization of theory of optimal spatial-time processing for the case of the reception of signals with both planar and spherical fronts, i.e., for the general case of the location of the observed objects and external interference sources in both the far field and the Fresnel zone of the receiving antennas[1].

In this treatment, the electromagnetic field of the signal has an additional parameter (as compared to the case of a plane wave), the curvature of the wave front, which can be employed as a source of information. For small sized ("point") signal sources, the curvature of the wave front is uniquely related to the range to the source. With suitable processing of the signal, this allows for the realization of the following additional capabilities, which are manifest more strongly, the greater the ratio of the dimensions of the antenna system to the range to the signal and interference sources, and the smaller the wavelength:

--The spatial resolution of the objects with respect to range, by virtue of the difference in the curvature of the wave fronts of the signals generated by them [2, 7, 8];

--The discrimination of the useful signals from interference generated by external sources, by means of selection based on the curvature of the wave fronts [9];

--The determination of the range of "point" signal sources based on the curvature of the wave fronts;

[1] For multiposition measurement systems, the antenna is understood to be the set of antennas of all the receiving stations.

In those active radar systems, where the range is measured based on the signal delay time, the use of a supplemental independent information source will permit increasing the precision of the range determination [10, 11, 12, 13, 14][2].

This paper is a survey of the basic principles and specific features of the optimum spatial-time processing of signals in the general case, including the processing of both plane and spherical waves, and a brief analysis is given of the potential characteristics of such processing (resolving power, noise immunity, and precision in the determination of the location of objects).

This analysis is based on both published and new results. To simplify the mathematical derivations, the treatment uses the example of a plane problem, where the antenna system is oriented along one of the coordinate axes, while the objects and interference sources being observed are located in the same plane. The basic governing laws ascertained using the plane problem example are also justified when the objects and interference sources being observed are positioned in three-dimensional space, as well as for antennas of any size (linear, planar, three-dimensional).

The Ambiguity Function of a Space-Time Signal and the Spatial Resolution Posibilities

A description of antenna systems and signals, geometric relationships. An antenna system with an overall dimension L and a center at the origin of the coordinates is oriented along the Ox axis (Figure 1). The geometry of the antenna system and the gain distribution in it are defined by the aperture function $\dot{I}(x)$ [3]. Basically, two forms of the functions $\dot{I}(x)$ will be considered: a function corresponding to a continuous linear aperture with uniform gain $|\dot{I}(x)|^2 = I$ when $|x| \leq L/2$; $|\dot{I}(x)|^2 = 0$ when $|x| > L/2$ and the discrete function $|I(x)|^2 = \sum_{i=1}^{n} \delta(x - x_i)$, , where x_i are the coordinates of the receiving elements. A continuous aperture for the case of reception in the Fresnel zone is somewhat of an idealization, however, such a representation of $\dot{I}(x)$ permits the derivation of the basic relationships in compact form, while the numerical results, as calculations show, practically coincide with the results obtained for an antenna array consisting of a large number of isotropic elements with spacings between adjacent elements less than λ. The discrete function $|\dot{I}(x)|^2$ is a sufficiently good description of an antenna array of isotropic (nondirectional) elements with an arbitrary number of

---

[2] Data on an active radar system are given in [15], in which the range measurement is based on the curvature of the wave front and the information on the time delay is not used.

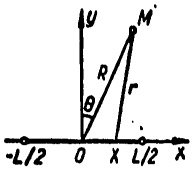

Figure 1.

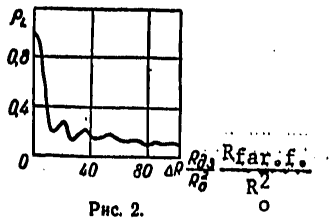

Рис. 2.

Figure 2.

elements and arbitrary spacings between them, as well as of the antenna systems of multiposition radio measurement systems under the same conditions and with relatively small antenna dimensions at the individual receiving stations.

Let the observed object take the form of a small (point) isotropic radiation source, located at the point M_0 with coordinates of R and Θ. The form of the signal radiated by the object (for the case of passive radar) or the sounding signal (in the case of active radar) is defined by the expression:

$$s_0(t) = \mathrm{Re}\{\dot{s}_0(t)\} = \mathrm{Re}\{\dot{U}(t)\, l^{j\omega t}\}, \tag{2}$$

where $\dot{U}(t)$ is the complex envelope of the signal. If the sounding signal is radiated from point 0, then when there are no distortions in it in the propagation process and the corresponding normalizing of the amplitude $s_0(t)$, the spatial-time signal being processed has the form:

$$\dot{s}(t, x) = a_0 l(x) \frac{R}{r(x)}\, \dot{s}_0\left(t - \frac{R + r(x)}{c}\right) l^{j\varphi_0}, \tag{3}$$

where ϕ_0 is the random initial phase which is uniformly distributed over the range $[0, 2\pi]$; r(x) is the range from the object to point x of the receiving antenna, equal to

$$r(x) = r(x, R, \theta) = \sqrt{R^2 + x^2 - 2Rx\sin\theta}, \tag{4}$$

a_0 is the amplitude of the received singal at the point x = 0. Under the same conditions, in the case of passive radar, if the time is read out with respect to the signal arriving at point 0, the signal being processed has the form:

$$\dot{s}(t, x) = a_0 l(x) \frac{R}{r(x)}\, \dot{s}_0\left(t - \frac{r(x) - R}{c}\right) l^{j\varphi_0}; \tag{5}$$

r(x) at values of the range R which considerably exceed the overall dimensions of the antenna system L, can be approximately represented by three terms of series (the Fresnel approximation):

$$r(x) = R - x\sin\theta + \frac{x^2\cos^2\theta}{2R} + \ldots \tag{6}$$

The near boundary of the field in which the Fresnel approximation can be used is determined from the condition where $\lambda/16$ does not exceed the value of the fourth term of series (6), and when $\Theta = 0$, the fifth term of the series.

$$R^2 \geqslant R^2_{бл1} = R_{дз}\frac{L\sin\theta}{2},\quad R^3 \geqslant R^3_{бл2} = R_{дз}\frac{L^2|1-5\sin^2\theta}{16}. \tag{7}$$

The region of the location of the objects being observed, $R_{бл}$ [R_{near}] $\leq$ $\leq R \leq R_{дз}$ [$R_{far\ field}$], where it is necessary to take into account the sphericity of the wave fronts and the Fresnel approximation can be used, we shall call the Fresnel region.

The ambiguity function of a space-time signal. Let two observed objects (signal sources) be positioned at points having coordinates of (R_1, Θ_1) and (R_2, Θ_2). Taking formulas (2), (3) and (5) into account, and neglecting the lack of equality of the amplitudes of the signal at the different points in the antenna system, something which is permissible when $R_{1,2} > L$ [16], the range and direction ambiguity functions for the case of active and passive radars will have the following forms respectively [6]:

$$\dot{\rho}(R_1, \theta_1, R_2, \theta_2) = \frac{\int_{-\infty}^{\infty} |\dot{I}(x)|^2 \dot{\rho}_\tau\left(\frac{r_1 + R_1 - r_2 - R_2}{c}\right)\exp j\frac{2\pi}{\lambda}(r_1 + R_1 - r_2 - R_2)\,dx}{\int_{-\infty}^{\infty} |I(x)|^2\,dx}, \tag{8}$$

$$\dot{\rho}(R_1, \theta_1, R_2, \theta_2) = \frac{\int_{-\infty}^{\infty} |\dot{I}(x)|^2 \dot{\rho}_\tau\left(\frac{r_1 - R_1 - r_2 + R_2}{c}\right)\exp j\frac{2\pi}{\lambda}(r_1 - R_1 - r_2 + R_2)\,dx}{\int_{-\infty}^{\infty} |I(x)|^2\,dx}, \tag{9}$$

where $\dot{\rho}_\tau(\tau)$ is the normalized complex autocorrelation function of signal (2); r_1 and r_2 are the distances from the signal sources to the point x of the antenna system.

In (9), the argument $\dot{\rho}_\tau$ is the difference in the time shifts of the signals received by the antenna system at the points x and 0. For the case of not very large antenna system dimensions (or a rather narrow spectral bandwidth Δf_c), the following conditions are observed

$$\frac{r_2 - R_2}{c} - \frac{r_1 - R_1}{c} \ll \frac{1}{\Delta f_c};\quad \rho_\tau \simeq 1 \tag{10}$$

and the ambiguity function (9) does not depend on the wave form of the signal $s_0(t)$. We shall introduce the following symbols: $\Delta R = R_1 - R_2$ is the difference in the ranges of the objects being resolved; $R_0 = \sqrt{R_1 R_2}$ is the mean geometric value of the ranges. Then, in case directional resolution is impossible ($\Theta_1 = \Theta_2 = \Theta$), taking approximation (6) into account, the expressions

for the range ambiguity functions for active (8) and passive (9) radar can be represented in the form

$$\rho(\Delta R, R_0, \theta) = \frac{\left|\int_{-\infty}^{\infty} |\dot{I}(x)|^2 \dot{\rho}_\tau \left(2\frac{\Delta R}{c} + \frac{x^2 \Delta R}{2cR_0^2}\cos^2\theta\right) \exp j\frac{2\pi}{\lambda}\left(2\frac{\Delta R}{c} + \frac{x^2\Delta R}{2cR_0^2}\cos^2\theta\right) dx\right|}{\int_{-\infty}^{\infty} |\dot{I}(x)|^2 dx}, \quad (11)$$

$$\dot{\rho}(\Delta R, R_0, \theta) = \left|\int_{-\infty}^{\infty} |\dot{I}(x)|^2 \dot{\rho}_\tau \left(\frac{x^2\Delta R}{2R_0^2 c}\cos^2\theta\right) \exp j\frac{2\pi}{\lambda}\left(\frac{x^2\Delta R}{2cR_0^2}\cos^2\theta\right) dx\right| \Big/ \int_{-\infty}^{\infty} |\dot{I}(x)|^2 dx. \quad (12)$$

As follows from (11), in the case of active radar, the resolving power with respect to range is due to two factors:

--The resolution with respect to the delay time (time resolution), determined by the $2\Delta R/c$ term in the $\dot{\rho}_\tau$ argument (when (10) is met, the values of the function $\dot{\rho}_\tau$ are determined by this term alone);

--The resolution due to the difference in the curvature of the wave fronts of the signals (spatial resolution).

In the case of passive radar, the range resolving power is due only to the spatial resolution. Formula (12) shows that the range resolving power due to the curvature of the wave front of the signals increases with an increase in the square of the ratio of the overall dimension of the antenna system L to the distance to the objects being resolved R_0, with a widening of the signal spectrum and a decrease in the wavelength. For a linear antenna of length L with uniform gain, if condition (10) is met, (12) yields the following [2]:

$$\rho_L(\Delta R, R_0, \theta) = C(\sqrt{a})/\sqrt{a}, \quad (13)$$

where $C(x) = \int_0^x \cos\pi\frac{t^2}{2}\,dt$ is a Fresnel cosine integral, $a = \Delta R L^2 \cos^2\theta/(2\lambda R_0^2)$.

The graph of the function $\rho_L(\Delta R, R_0, \theta)$, determined by (13), is shown in Figure 2. The width of this function at the 0.5 level is determined by the expression

$$\Delta R_{0.5} \simeq \frac{8R_0^2}{L^2\cos^2\theta}\lambda = 16\,R_0^2/R_{\text{ан}}. \quad (14)$$

Formula (14) shows that in systems with narrow band signals, resolution with respect to the curvature of the wave front can be effective only at ranges significantly less than the far field radius of the receiving antenna system. The latter condition is usually met for multiposition radio systems. In such radio systems, the values of the range R_0 are of the same order of magnitude as the overall dimensions of the antenna system L [5]. In this case, the range resolution interval runs to units or tens of wavelengths, i.e., an extremely high spatial resolution can be achieved. The failure to meet condition (10) leads to an additional improvement in the resolution with respect to the curvature of the front.

Optimal Spatial-Time Processing and the Discrimination of Signals from Interference

We shall consider signal processing for the case of active radar with a small isotropically reradiating target, located at a point with coordinates of (R, θ) (Figure 1). The following results, as applied to the spatial processing of the signals, are also justified for the case of passive radar for small radiation sources. The signal (3) is received by the antenna against a background of internal antenna system noise with a spectral density of N_0, which is uncorrelated at different points in the antenna system, as well as against a background of noise generated by an internal, small isotropic source of gaussian white noise, located at point M_n having coordinates of R_n and θ_n. The correlation functions of the internal and external interference at the antenna input have the form:

$$B_{BH}(t_1, t_2, x_1, x_2) = \frac{N_0}{2}\delta(x_1 - x_2)\delta(t_1 - t_2);\ B_{\text{п}}(t_1, t_2, x_1, x_2) = \\ = \frac{N_1}{2r_{n1}r_{n2}\int_{\Sigma} r_n^{-2}dx}\delta\left(t_1 - t_2 - \frac{r_{n1} - r_{n2}}{c}\right), \qquad (15)$$

[$B_{BH} = B_{internal}$] where N_1 is the spectral noise power density of the external source in the antenna aperture; r_{n1} and r_{n2} are the distances from the noise source to the points x_1 and x_2 of the antenna system, determined from (4).

Signal processing algorithms. When receiving spatial-time signals with a random initial phase against a background of gaussian noise, the absolute value of the correlation integral of [1] is taken as the output of the optimal (in the sense of a criterion of the probability ratio) signal processing system:

$$Z = \frac{1}{2}\left|\int_{(T)}\int_{(L)} \dot{u}(t, x)\,\dot{\sigma}^{*}(t, x)\,dtdx\right|, \qquad (16)$$

where $\dot{u}(t, x)$ is an additive mixture of the signal and interference; $\dot{\sigma}(t, x)$ is the reference signal which determines the signal processing algorithm; (T) and (L) are the time and space intervals, in which the signal processing is accomplished. The reference signal is defined by the relation:

$$\dot{\sigma}(t, x) = \int_{(T)} \int_{(L)} \Theta(t, t_1, x, x_1)\, \dot{s}(t_1, x_1)\, dt_1 dx_1, \qquad (17)$$

where s(t, x) is the useful signal, while $\Theta(t, t_1, x, x_1)$ is the inverse correlation function of the interference, defined from the integral equation:

$$\int_{(T)} \int_{(L)} \Theta(t_2, t_1, x_2, x_1) B(t, t_1, x, x_1)\, dt_1 dx_1 = \delta(t - t_2)\, \delta(x - x_2), \qquad (18)$$

where $B(t, t_1, x, x_1) = B_{BH}(t, t_1, x, x_1) + B_{\Pi}(t, t_1, x, x_1)$ is the correlation function of the interference at the antenna input. For a linear antenna with uniform gain, the reference signal which satifies equation (17) assumes the form:

$$\sigma(t, x) = \frac{2}{N_0} \left\{ \frac{R}{r(x)} s_0\left(t - \frac{R + r(x)}{c}\right) - \frac{N_1}{N_1 + N_0} \frac{1}{r_0(x) \int_{(L)} r_0^{-2}(x_2)\, dx_2} \times \right.$$

$$\left. \times \int_{(L)} \frac{R}{r(x_1) r_0(x_1)} \dot{s}_0\left(t - \frac{R + r(x_1) - r_0(x_1) + r_0(x)}{c}\right) dx_1, \right. \qquad (19)$$ (19)

and for the i-th receiving element of a discrete antenna system (antenna array):

$$\dot{\sigma}_i(t) = \frac{2}{N_0} \left\{ \frac{R}{r_i} \dot{s}_0\left(t - \frac{R + r_i}{c}\right) - \sum_{k=1}^{n} \Delta_{ik} \frac{R}{r_k} \dot{s}_0\left(t - \frac{R + r_k - r_{nk} + r_{ni}}{c}\right) \right\}, \qquad (20)$$

where $\Delta_{ik} = N_1 \left[r_{nk} r_{ni} (N_1 + N_0) \sum_{l=1}^{n} r_l^{-2} \right]^{-1}$.

The first terms on the right side of expression (20) and (19) describe processing matched to the received useful signal (3). In the following, we shall call spatial-time processing using such a reference signal matched processing. This processing is optimal only in the absence of noise generated by an external source. With matched processing, the antenna system is "focused" with respect to range and direction. The second terms in (19) and (20), subtracted from the first, provide for optimal compensation of external interference. The essence of optimal spatial-time processing in the presence of internal and external noise is more clearly seen in the case where expansion (6) can be used, and the signal is a narrow band one in the spatial-timewise sense (the correlation time of the signal $1/\Delta f_c$ is many times greater than the maximum value of the time shift between the signal values at the extreme points of the antenna system). For the case of range values which exceed the overall dimensions of the antenna system, one can neglect the inequality of the amplitudes of the signals at different points in the antenna. Then formula (19) assumes the form:

$$\dot{\sigma}(t, x) = \frac{2}{N_0} \dot{U}\left(t - \frac{2R}{c}\right) e^{j\omega_0\left(t - \frac{2R}{c}\right)} \left\{ \exp\left[j\omega_0 \left(\frac{x \sin\Theta}{c} - \frac{x^2 \cos^2\Theta}{2Rc} \right) \right] - \right.$$

$$\left. - \frac{N_1}{N_1 + N_0} \dot{\rho}_L(R_n, \Theta_n, R, \Theta) \exp\left[j\omega_0 \left(\frac{x \sin\Theta_n}{c} - \frac{x^2 \cos^2\Theta_n}{2R_n c} \right) \right] \right\}, \qquad (21)$$

where

$$\dot{\rho}_L(R_1, R_2, \Theta_1, \Theta_2) = \frac{1}{L}\int_{-L/2}^{L/2} \exp\left\{ j\frac{2\pi}{\lambda}\left[x(\sin\Theta_1 - \sin\Theta_2) - \right.\right.$$

$$\left.\left. - \frac{x^2}{2}\left(\frac{\cos^2\Theta_1}{R_1} - \frac{\cos^2\Theta_2}{R_2}\right)\right]\right\} dx. \qquad (22)$$

The expression which defines the form of the reference signal for the antenna array is determined on analogy with (21), substituting x_1 for x. It is not difficult to see from (21) that with spatial-narrow band signals, time and spatial processing are separated: the factor in front of the curly braces determines the optimum timewise processing of a signal, and the expression in the curly braces determines its spatial processing, which reduces to the matched spatial processing of the useful and interference signals, and the subtraction from the results of the first operation of the result of the second. The subtraction is carried out with the weighting factor $N_1\dot{\rho}_L(R_\pi, \Theta_\pi, R, 0)/(N_0 + N_1)$, defined by the mutual positioning of the target and the noise source, as well as the relationship of the external and internal noise intensity. Where several external noise sources are present, matched spatial processing should be carried out for each source, just as in (19), with weighting coefficients which depend on the relationship of the intensities of the noise sources and their mutual arrangement [9]. Usually, the coordinates and intensities of the noise sources areunknown beforehand, and for this reason, they should be determined by the processing system in the process of generating the reference signal. The design of such processing systems is possible by means of using the principles analyzed in [2, 17].

The suppression of noise generated by external sources. The effectiveness of the suppression of noise generated by external sources can be evaluated in terms of the signal to noise ratio at the output of the processing system. The power signal to noise ratio for the case of spatial-time signal processing is equal to [1]:

$$q^2 = \frac{1}{2}\left|\int_{(T)}\int_{(L)} \dot{s}(t, x)\dot{\sigma}(t, x)\, dt dx\right|. \qquad (23)$$

To estimate the level of external noise suppression, we shall introduce the following coefficients:

$$k = q^2/q_0^2; \qquad l = q^2/q_{\text{пл}}^2, \qquad (24)$$

where q^2 is the output signal to noise ratio for the case of optimum processing of a signal with aspherical front against a background of internal and external noise; $q^2_{\text{пл}}$ is the same for the optimal processing of a signal with a plane wave front under the same conditions; q_0^2 applies in the absence of external noise. The coefficient k indicates the degradation of the output signal to noise ratio by virtue of the presence of external noise; the coefficient l is the level of suppression of external noise through the use of information on the curvature of the wave fronts.

In the optimal processing of narrow band signals in a linear antenna of length L, formula (23), taking (21) into account, yields the following [9]:

$$k = 1 - \frac{N_1}{N_1 + N_0} |\dot{\rho}_L(R_n, \Theta_n, R, \Theta)|^2, \quad l = \left(1 + \frac{N_1}{N_0}\right) k. \tag{25}$$

The values of the coefficients k and l are shown in Figures 3a and 3b (the solid lines) as a function of $\gamma = \left|\frac{R_{дз}}{R} - \frac{R_{дз}}{R_n}\right|$, , where $R_{дз}$ is the far field radius of (1), for the case where the angular coordinates of the noise source and the target coincide ($\Theta_п = \Theta$), and gating of the external noise is possible only through the difference in the curvature of their wavefronts. As follows from Figure 3, with a significant difference in range between the signal and noise sources ($\gamma >> 1$) $k \approx 1$, i.e., the external noise can be suppressed almost completely. In this case, the advantage gained in the signal to noise ratio as compared to the case of processing a plane wave l is approximately equal to the ratio of the spectral densities of the external and internal noise at the antenna aperture. The gain falls off in step with a decrease in the curvature of the wave front.

It was noted above that the realization of optimal spatial-time processing of signals where external noise sources are present is rather complicated. For this reason, it is of interest to assess the possibilities of suppressing external noise for the case of simpler (from a design viewpoint) matched processing. In this case, the coefficients k and l are defined as:

$$k = \frac{N_0}{N_0 + N_1 |\dot{\rho}_L(R_n, \Theta_n, R, \Theta)|^2}, \quad l = \left(1 + \frac{N_1}{N_0}\right) k. \tag{26}$$

The values of k and l with matched processing for the case of $\Theta_п = \Theta$ are shown in Figures 3a and 3b by the dashed line. A comparision of these curves with the curves for the case of optimal processing shows that at extremely small ($\gamma \approx 0$) and extremely large ($\gamma > 20$) curvatures of the wave front, matched processing provides for approximately the same degree of external noise suppression as optimal processing, while in intermediate cases ($1 < \gamma < 20$), optimal processing is more effective.

Figure 4 illustrates the suppression of external noise for the case of optimal spatial-time processing in multiposition radio systems, where the number of receiving points is small, while the spacings between them are >> λ. The curves are plotted for the case where there is no gating with respect to direction ($\Theta_п = \Theta$), while the noise source is located in the far field ($\gamma \approx R_{ff}/R$). The dashed lines apply to a three-position system ($x_1 = -0.45$ L, $x_2 = 0$, $x_3 = 0.55$ L), and the solid lines apply to a five-position system ($x_1 = -0.45$ L, $x_2 = -0.2$ L, $x_3 = 0$, $x_4 = 0.25$ L, $x_5 = 0.55$ L). The curves in Figure 4 attest to the fact that in multiposition systems, the input signal/noise ratio expressed as a function of $\gamma = R_{ff}/R$ is of an oscillating nature. An increase in the number of receiving positions leads to a smoothing of the oscillations.

For the case of active radar:

$$\sigma_R^2 = \frac{c^2}{\omega_0^2 q_0^2}\left\{4\left(\frac{\Pi_э}{\omega_0}\right)^2\left[1+\frac{L_2^2}{2R^2\left(\frac{\Pi_э^2}{\omega_0^2}+1\right)}\left(\cos^2\Theta+\frac{\Pi_э^2}{\omega_0^2}+\frac{\Pi_э^2}{\omega_0^2}\sin^2\Theta\right)+\right.\right.$$

$$\left.\left.+\frac{L_4^4}{16R^4}\cos^2\Theta(7-31\sin^2\Theta)\right]+\frac{L_4^4-L_2^4}{4R^4}\cos^4\Theta\right\}^{-1}. \qquad (28)$$

In formulas (27) and (28), L_2^2 and L_4^4 are the normalized second and fourth moments of the square of the aperture functions $|\dot{I}(x)|^2$ [1, 3], determined by the geometry of the antenna system and the gain distribution in it; q_0^2 is the signal/noise ratio; c is the speed of light; $\Pi_э^2$ is the square of the equivalent width of the signal spectrum, defined as the second central moment of the spectrum. The formulas are derived using the approximate expansion (6).

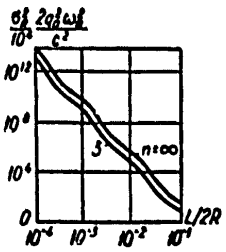

Figure 5.

For the case of range measurement based only on the curvature of the wave front, the measurement error as follows from (27), is proportional to the wavelength λ and the square of the ratio of the range R to the overall size of the antenna L, and the error depends slightly on the spectral width of the signal. Shown in Figure 5 is the normalized dispersion of the range measurement as a function of the ratio L/2R for a linear antenna of length L, with a uniform gain distribution, and for an equally spaced antenna array of the same length consisting of three elements where $(\Pi_э/\omega_0)^2 \ll 1$.

In active radar, for the case of optimal spatial-time processing of the signals, the range is determined by means of the joint utilization of the information on the delay time and the curvature of the wave front of the signals. To estimate the influence of wave front curvature information on the precision of range measurement, shown in Figures 6a and 6b are the ratio of the dispersions of the range estimate for the case of optimal spatial-time processing of the signals (σ_R^2) and for the case of measurement based on the delay time (σ_{R0}^2) for a linear antenna of length L (Figure 6a) and for an equally spaced antenna array of the same length (Figure 6b). As can be seen from Figures 6a and 6b, the use of wave front curvature information permits a substantial increase in the range measurement precision when $L/R > L/R_{bound} \approx 2\sqrt{\Pi_э/\omega_0}$.

For example, with a relative spectral width of $\Pi_э/\omega_0 = 10^{-6}$, the influence of the information on the curvature of the wave front begins to have a substantial effect at ranges of $R_2 \leq 10^3 L$. An analysis of Figures 4, 5 and 6a shows that for identical values of the output signal/noise ratio and identical overall dimensions of the antenna, the range measurement precesion when using "dispersed" antenna arrays is higher than when using antennas with a continuous

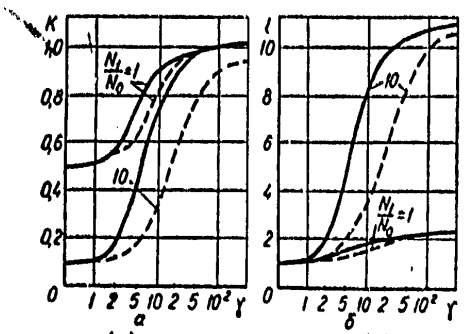

Figure 3.

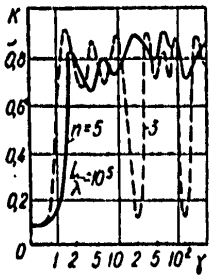

Figure 4.

Based on the values of the signal/noise ratio at the output of the processing system computed from formulas (19)--(23), the probability of detecting an object by means of the well-known detection curves can be determined. In this case, it is necessary to consider the fact that at small values of R/L, an increase in the range resolving power by virtue of resolution of the curvature of the wave front leads to an increase in the number of resolution elements in the scanning field, and consequently, to an increase in the false alarm probability.

Determining the Position of Objects and Their Parameters of Motion

The possibility of determining range based on the curvature of a wave front arises with spatial-time processing of signals with spherical wave fronts. In passive radar systems, this is the sole primary source of information concerning the range; in active radar systems, the information on the wave front curvature can be employed in conjunction with the information on the delay time of the signals to increase the precision in determining the location of objects, and in some cases, it can be used independently [15]. For the case of interference in the form of gaussian white noise, which is not correlated at the different points in the receiving antenna system, as well as for large signal/noise ratios, the precision in the estimation of the range R using the maximum probability method is characterized by the following expression:

For the case of passive radar

$$\sigma_R^2 = \frac{4R^4c^2}{q^2\omega_0^2\cos^4\Theta_0}\left\{\left(\left(\frac{\Pi_0}{\omega_0}\right)^2+1\right)L_1^4 - L_2^4\right\}^{-1}; \tag{27}$$

aperture, and becomes higher the smaller the number of elements of the array. However, for large values of L/λ, a reduction in the number of elements of the array can lead to ambiguity in the measurements which can be eliminated by means of expanding the spectrum of the signal being processed. The requirements placed on the signal spectrum to eleiminate measurement ambiguity in the angular coordinates when using "dispersed" arrays in the general case of the positioning of the objects being observed do not differ substantially from the requirements which are set when the objects are located in the far field of the antenna array. The ambiguity phenomenon of range measurements arises in the spatial-time processing of signals with a spherical front. It can be shown that ambiguity in the range measurement can arise when receiving signals with a linear, equally spaced antenna array containing n elements, where $n < [1/4]\ (R_{ff}/R + 3)$. The ambiguity is eliminated if the signal spectrum width Δf_c meets the condition:

$$\Delta f_c/f_0 > \frac{n-2}{4(n-1)^2}\left(\frac{L}{R}\cos\theta\right)^2. \tag{29}$$

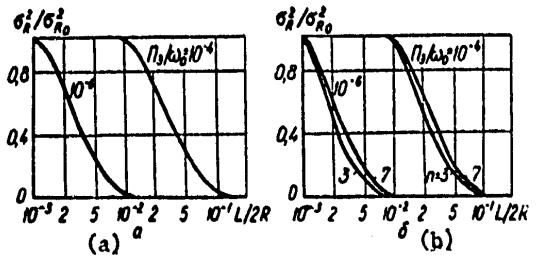

Figure 6.

Figure 7.

In paper [11], the potential precision in the estimate of coordinates is analyzed for the case of an antenna of any size. A comparison of the results obtained in this paper for a circular antenna, with those results given above for a linera antenna shows that for the case of equal overall size, the advantage gained in precision by virtue of using information on the wave front curvature is approximately the same for both antennas.

An analysis of the precision in estimating the angular coordinate of an object in the general case shows that when receiving signals with spherical wave fronts, the potential precision of the determination of directions is practically the same as when receiving signals with plane wave fronts.

Ignoring the wave front curvature in spatial-time processing of signals can lead to a substantial degredation of the signal/noise ratio and the range measurement precision. Thus, when $R = 0.02\ R_{ff}$, the signal/noise ratio falls off by tens of times [11]. The range measurement precision, as a result of failing to take into account the information contained in the curvature of the wave front, for $R = 25L$ and $L/\lambda = 100$, decreases by ten times when $\Pi_э/\omega_0 = 10^{-3}$ and by 100 times when $\Pi_э/\omega_0 = 10^{-6}$ [18].

The potential possibilities for increasing the accuracy of multiposition radio systems operating in the Fresnel zone can be illustrated by means of comparing the precision of range measurement in a range difference (hyperbolic) radio naviagation system [6] and in a system with the same arrangement of the receiving stations, which carries out the optimal spatial-time processing of the signal. Shown in Figure 7 is the ratio of the dispersions of the range estimate σ_h^2 in a two-base hyperbolic system with receiving stations at the points $x_1 = L/2$, $x_2 = 0$, $x_3 = -L/2$, and in a system which realizes the optimal processing of the signals received at the same stations: σ_{opt}^2 (σ_h^2 was determined on the basis of the relationships given in [6], and the values of σ_{opt}^2 were determined from formula (29) twice. It can be seen from Figure 7 that the precision which can be attained in hyperbolic radio navigation systems is extremely for from the potential accuracy obtainable with optimal coherent processing of the signal.

The relationshipsggiven above were derived with the assumption that the signal/noise ratio is rather high, and the range estimate is reliable, i.e., the probability of anomolous errors is neglectibly small. With small values of the parameter R/L, the resolving power with respect to range increases sharply by virtue of the resolution based on the curvature of the wave front, and consequently, the probability of anomolous errors also increases. In this case, higher values of the signal to noise ratio can be necessary to assure reliability of the estimate than is true of the case of range measurement based only on the signal delay time. An analysis of this phenomenon is given in the literature [19], the results of which show that for signal to noise ratios of $q_0^2 \leq 20$, the increase in anomolous errors must be taken into account at relatively small values of the range (as compared to the dimensions of the antenna system) and at a relatively small signal spectral width (for $\Pi_э/\omega_0 = 10^{-3}$--10^{-4} when $R < (1\text{--}3)L$, for $\Pi_э/\omega_0 = 10^{-5}$--10^{-6} at $R < (10\text{--}30)L$. In many cases, the measurement systems should determine the parameters of object motion, i.e., the derivatives of the coordinates, along with the coordintes of the objects. The potential accuracy of the joint estimation of the coordinates and their derivatives for the case of spatial-time processing of signals in the general case was investigated in [12], where it was shown that taking the curvature of the signal wave front into account has practically no influence on the precision of the simultaneous estimation of the angular coordinate and its derivative. With the simultaneous estimation of the range and its derivative, the potential precision of the estimate of the radial velocity in the Fresnel zone when using signals without frequency modulation is the same as for the far field, and for signals with frequency modulation, can be substantially higher. This is explained by the fact that for FM signals, the estimates of the range and velocity are correlated due to the specific dependence between the frequency and time shifts for these signals. In determining range, the use of the information on wave front curvature, which is not related to the signal time shift, simultaneously boosts the precesion of the range estimates and weakens the correlation between the velocity and range estimates. For this reason, increasing the precision of the radial velocity estimate is more important, the smaller the R/L ratio and the narrower the signal spectrum.

The expressions given above, which were derived for the general case of the positioning of the targets and the noise sources, includes as a special case, the relationships described in the literature for spatial-time processing of signals with plane wave fronts.

Conclusion

Thus, based on the analysis carried out above for the main features and the potential characteristics of spatial-time processing of signals in the general case, which includes the processing of both plane and spherical waves, the conclusion can be drawn that with spherical waves, it is possible to achieve a higher resolving power, noise immunity and precision in the radio system. When estimating the capability of achieving these potential characteristics, along with the difficulties of the engineering design for coherent processing, it is necessary to likewise consider the fundamental limitations placed due to radio wave propagation conditions and the characteristics of the radiation of the objects being observed. These factors can degrade the system characteristics as compared to the potentially possible ones cited above, but cannot completely eliminate the advantages which result from information on the curvature of the signal wave fronts.

BIBLIOGRAPHY

1. Fal'kovich S.Ye., "Otsenka parametra signalov" ["Estimating a Signal Parameter"], Moscow, Sovetskoye Radio Publishers, 1970.

2. Shirman Ya.D., "Razresheniye i szhatiye signalov" ["Signal Resolution and Compression"], Moscow, Sovetskoye Radio Publishers, 1974.

3. Urkovits, "Tochnost' otsenki uglovykh koordinat v radiolokatsii i gidrolokatsii po metody maksimal'nogo pravdopodobiya" ["The Precision of the Estimation of Angular Coordinates in Radar and Sonar using the Maximum Plausibility Method"], ZARUBEZHNAYA RADIOELEKTRONIKA [FOREIGN RADIOELECTRONICS], 1964, No 10.

4. Kontorov D.S., Golubev-Novozhilov Yu.S., "Vvedeniye v radiolokatsionnuyu sistemotekhniku" ["Introduction to Radar Systems Engineering"], Moscow, Sovetskoye Radio Publishers, 1971.

5. "Spravochnik po radiolokatsii" ["Radar Handbook"], Edited by M.I. Skolnik, Moscow, Sovetskoye Radio Publishers, 1978, 4.

6. Skiba N.I., "Sovremennyye giperbolicheskiye sistemy dal'ney navigatsii" ["Modern Hyperbolic Long Range Navigation Systems"], Moscow, Sovetskoye Radio Publishers, 1967.

7. Dulevich V.Ye., et al., "Teoreticheskiye osnovy radiolokatsii" ["The Theoretical Fundamentals of Radar"], Moscow, Sovetskoye Radio Publishers, 1964.

8. Reutov A.P., Mikhaylov B.A., Kondratenkov G.S., Boykov B.V., "Radiolokatsionnyye sistemy bokovogo obzora" ["Side Scan Radar Systems"], Moscow, Sovetskoye Radio Publishers, 1970.

9. Kremer I.Ya., Pon'kin V.A., "Prostranstvenno-vremennaya obrabotka signalov v zone Frenelya" ["Spatial-Time Signal Processing in the Fresnel Zone"], RADIOTEKHNIKA I ELEKTRONIKA, 1977, 22, No 1, p 72.

10. Kremer I.Ya., Nakhmanson G.F., Sidorik Ye.G., "O potentsial'noy tochnosti otsenki mestopolozheniya tseli pri passivnoy lokatsii na fone prostranstvenno-raspredelennykh pomekh" ["On the Potential Precision of an Estimate of Target Location with Passive Radar against a Background of Spatially Distributed Interference" IZV. VUZOV - RADIOELEKTRONIKA [PROCEEDINGS OF THE HIGHER EDUCATIONAL INSTITUTES - RADIO ELECTRONICS], 1977, 20, No 9, p 40.

11. Kremer A.I., Trifonov A.P., "Predel'naya tochnost' otsenki koordinat tochechnoy tseli" ["The Maximum Precision in the Estimate of the Coordinates of a Point Target"], RADIOTEKHNIKA I ELEKTRONIKA, 1977, 22, No 8, p 1,607.

12. Kremer A.I., Trifonov A.P., "Predel'naya tochnost' sovmestnoy otsenki koordinat i ikh proizvodnykh radiolokatsionnymi metodami" ["The Maximum Precision of the Simultaneous Estimation of Coordinates and Their Derivatives using Radar Methods"], RADIOTEKHNIKA I ELEKTRONIKA, 1978, 23, No 1, p 67.

13. Karavayev V.V., Sazonov V.V., "O tochnosti otobrazheniya ob"yekta v golografii" ["On the Accuracy of the Representation of an Object in Holography"], RADIOTEKHNIKA I ELEKTRONIKA, 1970, 15, No 11, p 2,396.

14. Gershman S.G., Shikalov A.A., "Otsenka potentsial'noy tochnosti izmereniya rasstoyaniya do nepodvizhnogo istochnika shuma" ["An Estimate of the Potential Precision in the Measurement of the Range to a Stationary Noise Source"], AKUSTICHESKIY ZHURNAL, 1977, 23, No 2, p 249.

15. Iziduka K., Ogura Kh., Yan' Dzh.L., Nguyen V.Kh., Uidmark Dzh.R., "Radiolokator na baze golograficheskoy matritsy" ["A Radar Designed Around a Holographic Matrix"], TIIER, 1976, 64, No 10, 45.

16. Kremet A.I., Trifonov A.P., "Vliyaniye razmerov antenny na pomekhoustoychivost' priema prostranstvenno-vremennogo signala" ["The Influence of Antenna Dimensions on the Reception Noise Immunity of a Spatial-Time Signal"], IZV. VUZOV - RADIOELEKTRONIKA, 1977, 20, No 8, p 102.

17. Burakov V.A., Zorin L.A., Ratynskiy M.V., Shishkin B.V., "Adaptivnyye obrabotki signalov v antennykh reshetkakh" ["Adaptive Signal Processing in Antenna Arrays", ZARUBEZHNAYA RADIOELEKTRONIKA, 1976, No 8, p 35.

18. Kremer A.I., Trifonov A.P., "Sravneniye tochnosti optimal'noy i kvazioptimal'noy otsenok dal'nosti pri lokatsii v zone Frenelya" ["A Comparison of the Precision of Optimal and Quasioptimal Estimates of the Range with Fresnel Zone Radar"], IZV. VUZOV - RADIOELEKTRONIKA, 1978, 21, No 3, p 92.

19. Kremer A.I., Trifonov A.P., "O porogovykh effektakh pri otsenke mestopolozheniya tseli v zone Frenelya" ["On Threshold Effects when Estimating the Location of a Target in the Fresnel Zone"], RADIOTEKHNIKA I ELEKTRONIKA, 1978, 23, No 3, p 629.

8225
CSO:1870

ELECTRONICS AND ELECTRICAL ENGINEERING

UDC 537.862:621.385.6

THE SYNCHRONOUS EXCITATION OF THE PRIMARY HARMONIC OF A FIELD WITH A PERIODIC STRUCTURE BY AN INCIDENT NONRELATIVISTIC FLOW

Kiev IVUZ RADIOELEKTRONIKA in Russian Vol 21 No 11, Nov 78 pp 109-113

[Article by G.A. Alekseyev, A.Ya. Kirichenko and V.I. Mikhaylov, manuscript received 14 Nov, 1977]

[Text] The problem of exciting a flat periodic structure of the "comb" type with a wide, premodulated electron flow, incident to the surface of the structure at a large angle, is analyzed. The condition for the synchronous excitation of spatial harmonics is also analyzed for the case of the sequential interaction of the electrons with the transverse component of the electric field. The theoretical analysis is carried out within the framework of a specified current level procedure. The possibility of synchronously exciting the primary harmonic of the resonant field of the comb with a nonrelativistic electron flow incident at a large angle is experimentally confirmed.

The interaction of electron flows with the higher spatial harmonics of the field of a periodic structure, or relativistic electron flows are usually employed to overcome difficulties in the scale modeling when designing O-type microwave generators in the shortwave band [1]. The trends cited here are due to the fact that with electron excitation of distributed electrodynamic structures, as a rule, the motion and bunching of the electron flow in the direction of wave propagation are usually employed i.e., in a longitudinal direction, while the interaction of the electrons is realized with the longitudinal component of the electric field [sic].

However, the transition to operation at the higher spatial harmonics of the field leads to a considerable degradation of the energy exchange between the electron flow and the high frequency field, due to the sharp reduction in the coupling resistance. In step with the shortening of the wavelength of the generated wave, difficulties also arise which are related to the necessity of guiding intense electron flows close to the periodic structure, parallel to its surface.

One of the methods of overcoming these difficulties can be the use of synchronous electron excitation in O-type devices of waveguide distributed systems with an aggregate of charges which are phased modulated in the direction of wave propagation, where these charges move transversely with respect to the system, and there is a short term local mechanism for their interaction with the transverse component of the electric field. Various configurations for the use of such sequential interaction of electrons with the high frequency field to excite electromagnetic waves were proposed and analyzed in the literature [2 - 6].

In particular, the synchronous excitation of a plane periodic structure can be accomplished with a wide premodulated electron flow, where the generated bunches are incident to its surface at a specified angle (Figure 1).

The synchronous excitation condition, working from which the optimum value of the angle $\phi = \phi_0$ is defined, is in this case the condition of equality of the velocity of the intersection point of the surface of the structure with the front of the incident bunch ,and the phase velocity v_{nm} of the excited m-th spatial harmonic of the field at a frequency of $n\omega$:

$$\frac{v_e}{\sin \varphi_0} = v_{nm}. \qquad (1)$$

Here v_e is the electron velocity of the flow; ω is the modulation frequency.

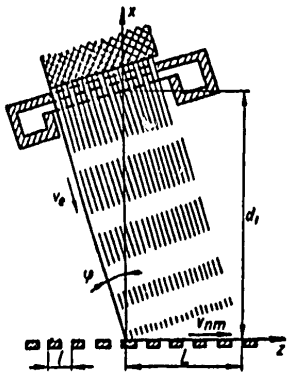

Figure 1.

The velocity $v_e/\sin\phi_0$, defined in [3] as the phase velocity of the sequence of particles, and in [5] as the velocity of the electron wave crest, because of smallness of the angle ϕ_0 can be chosen rather large. and even exceed the velocity of light in a vacuum. In this case, as noted in [5], there arises the possibility of the interaction of electron flows with fast electromagnetic waves. When using periodic structures though, there also arises the possibility of their excitation at the primary spatial harmonic ($m = 0$) at a nonrelativistic velocity of the electrons v_e and at rather high values of the phase velocity v_{n0}.

The case of the synchronous excitation of the primary harmonic of the field of a periodic comb type structure with a wide, incident, premodulated electron flow is treated in this paper.

An approximate theoretical description of synchronous excition, as applied to the configuration of Figure 1, can be serived within the framework of a specified current level procedure.

For the i_{nx} component of the current, bunched at a frequency of $n\omega$ in the drift space, following velocity modulation in the gap of a toroidal resonator with a voltage $U\sin\omega t$, for an arbitrary slope angle ϕ of the generated bunches, one can write:

$$i_{nx}(x, z, t) = 2i_0 J_n(nX)\cos\varphi\cos n(\omega t - \theta_0), \tag{2}$$

where i_0 is the linear current density at the input to the modulator; j_n is a Bessel function; $X = \mu\theta_0$ is the flow bunching parameter; θ_0 is the aperture angle. For the configuration considered here:

$$\theta_0(x, z) = \frac{\omega(d_1 + z\,\mathrm{tg}\,\varphi - x)\cos\varphi}{v_e}, \tag{3}$$

where d_1 is the distance from the periodic structure to the modulating resonator at the cross section $z = 0$. The parameter μ characterizes the velocity modulation level of the flow and is defined by well known expressions from kinematic or electron-wave analysis. When taking into account the action of space charge forces in the direction of flow travel, the parameter μ is equal to:

$$\mu = \frac{U}{2U_0} M \frac{\sin\left[\frac{\omega_p}{v_e}(d_1 + z\,\mathrm{tg}\,\varphi - x)\cos\varphi\right]}{\frac{\omega_p}{v_e}(d_1 + z\,\mathrm{tg}\,\varphi - x)\cos\varphi}, \tag{4}$$

where M is the parameter of velocity modulation; ω_p is the plasma frequency; $U_0 = (1/2)(m/e)v_e^2$ is the accelerating voltage.

In the case where $\phi = 0$, expressions (2) -- (4) correspond to the unidimensional theory of electron flow bunching in the drift space. For the m-th spatial harmonic of the resonant field of a comb type periodic structure, the interaction with which is considered here, one can use the expression:

$$E_{nmx} = -E^0_{nm}(z)\,e^{-\beta_{nm}x}\sin(n\omega t - \beta_{nm}z - \psi_0), \tag{5}$$

where $\beta_{nm} = n\omega/v_{nm}$; $E^0_{nm}(z)$ is the amplitude of the field harmonic at the level of the interaction system; ψ_0 is the constant phase shift with respect to the voltage in the resonator gap.

By making use of the slowness of the change in the function $J_n(nX)$ in the range $\Delta x \approx 1/\beta_{nm}$ (with the condition $\omega_p \ll \omega$), which is important for the integration, and by working from the linear nature of the rise in the amplitude $E^0_{nm}(z)$ with an optimum phase shift of $\psi_0 = (n\omega d_1/v_e) + \pi/2)$, one can derive the following approximation for the interaction power:

$$P_e \approx \int_0^L \int_0^{d_2 + z\,\mathrm{tg}\,\varphi} \overline{i_{nx}E_{nmx}}\,dx\,dz \approx -I_0 E^0_{nm}(L) J_n(nX_1) \times$$

$$\times \frac{\sin\beta_{nm}\rho L}{\beta_{nm}\rho L} \frac{\beta_{nm}}{\beta^2_{nm} + \left(\frac{n\omega}{v_e}\right)^2 \cos^2\varphi}. \tag{6}$$

here, $I_0 = i_0 L \cos\phi$ is the total beam current; X_1 is the bunching parameter of the flow in the plane of the periodic structure at $z = 0$; $\rho = 1 - (v_{nm}/v_e) \sin\phi$ is the desynchronization parameter.

It can be seen from (6) that the optimal conditions for the interaction of the electron flow with the spatial field harmonic are realized for the case $\rho = 0$, i.e., when condition (1) is met. In this case, the electrons interact in sequential fashion with the high frequency field, and there is synchronous excitation of the structure.

By equating the quantity P_e to the flow of power in the transmission line $P_{nm} = (E^0_{nm})^2/2\beta^2_{nm}K_{nm}$, where K_{nm} is the coupling resistance of the spatial harmonic at the frequency $n\omega$, we obtain the following expression for the amplitude of the field in the section $z = L$:

$$E^0_{nm}(L) = 2K_{nm}I_0 J_n(nX_1)\frac{\beta_{nm}}{1+\left(\frac{v_{nm}}{v_e}\right)^2\cos^2\varphi_0}. \qquad (7)$$

An analysis of (7) taking into account the coupling resistance K_{nm} as a function of the number of the spatial harmonic shows that due to the rapid decrease in K_{nm} with an increase in m, interaction with the primarly field harmonic is more effective (for the case of a fixed velocity v_e) where $v_e << v_{n0}$, then interaction with a higher spatial harmonic ($m \neq 0$) when $v_e \approx v_{nm}$.

In fact, the ratio of the coupling resistances at the primary and higher spatial harmonics is given by the expression [7]:

$$\frac{K_{nm}}{K_{n0}} = \left(\frac{v^2_{nm}\sin\frac{n\omega l}{2v_{nm}}}{v^2_{n0}\sin\frac{n\omega l}{2v_{n0}}}\right)^2, \qquad (8)$$

where l is the period of the structure.

It can be seen from a comparison of (8) and (7) that with an increase in m, K_{nm} falls off faster than the latter factor in (7) increases in this case.

The spacific features of the synchronous excitation of a comb type periodic structure with a wide incident electron flow, as applicable to the configuration of Figure 1, were analyzed experimentally. The beam width in the z direction was $4\pi/\beta_{n0}$. The angle of incidence $\phi = \phi_0$ was chosen at 17°. The excited microwave radiation at a frequency corresponding to the fourth time harmonic of the modulating signal (n = 4) was registered by a detecting receiver. The distance from the modulator to the comb d_1 at the cross-section $z = 0$ was chosen so that the amplitude of the i_n current harmonic was maximal in the plane of the periodic structure.

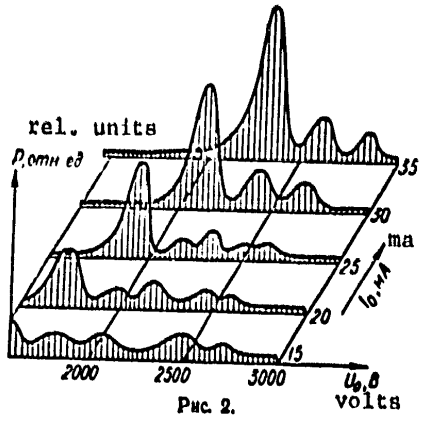

Рис. 2.

Figure 2.

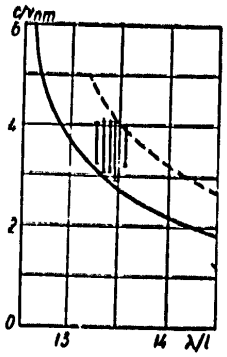

Рис. 3.

Figure 3.

The amplitude of the output signal is shown in Figure 2 as a function of the level of the accelerating voltage U_0 for various values I_0. It can seen from the Figure that the experimental function E_{n0} (U_0) is of a nonmonotonic nature with a number of maxima and minima. The primary voltage maximum corresponds to values of v_e at which the optimal value of the angle ϕ_0 is found close to 17°.

It can also be seen from Figure 2 that the radiation intensity at the primary maximum depends on the current level, something which is in agreement with expression (6). The position ofthe primary maximum is shifted in the direction of higher accelerating voltages with an increase in I_0, something which is related to the nature of the change in the function J_n (I_0) as a function of the space charges density.

The dispersion function of the position of the main maximum, which is shown in Figure 3, confirms that operation is realized at the primary spatial harmonic of the field (m = 0). The vertical straight lines in Figure 3 depict the experimental data. The solid curve represents the dispersion of the comb, which was obtained by calculation, while the dashed line represents the dispersion of the hot system when excited by a flow parallel to the surface of the periodic structure.

The investigations carried out here confirm the possibility of the effective excitation of a periodic structure with a premodulated incident electron flow. In this case, it proves possible to excite the periodic structure at the primary spatial harmonic, without turning to an increase in the accelerating voltages or using relativistic electron flows. To excite the primary spatial harmonic of the field of the comb used in this experiment by an electron flow moving parallel to the surface of the structure, an accelerating voltage an order of magnitude higher would have been required.

The synchronous excitation of periodic structures with a transverse flow of electrons can prove to be useful in both the design of generators (for example, frequency multipliers), and in the study of electrodynamic structures with retardations close to unity.

BIBLIOGRAPHY

1. Devyatkov N.D., Golant M.B., "Puti razvitiya elektronnykh priborov millimetrovogo i submillimetrovogo diapazonov dlin voln" ["Ways of Improving Millimeter and Submillimeter Wavelength Electronic Devices"], RADIOTEKHNIKA I ELEKTRONIKA, 1967, 12, No 11, p 1,973.

2. Mihran T.G., "The Duplex Traveling Wave Klystron", PIRE, 1952, 40, No 3, p 308.

3. Tetel'baum S.I., "Fazove fokusuvannya pri poperechniy modulyatsii shvidkosti" ["Phase Focusing During Transverse Flow Modulation"], DAN URSR [REPORTS OF THE UKRAINIAN ACADEMY OF SCIENCES], 1955, No 1, p 54. [sic].

4. Alekseyev F.A., Bliokh P.V., "Kogerentnoye tormoznoye izlucheniye protyazhennykh sgustkov" ["Coherent Braking Radiation of Extended Bunches"], IZV. VUZOV - RADIOFIZIKA [PROCEEDINGS OF THE HIGHER EDUCATIONAL INSTITUTES - RADIOPHYSICS], 1964, 7, No 6, p 1,064.

5. Bolotovskiy B.M., Ginzburg V.L., "Effekt Vavilova-Cherenkova i effekt Dopplera pri dvizhenii istochnikov so skorost'yu, bol'she skorosti sveta v vakuume" ["The Vavilov-Cherenkov Effect and the Doppler Effect with the Motion of Sources at a Velocity Greater than the Velocity of Light in a Vacuum"], UFN [USPEKHI FIZICHESKIKH NAUK - ADVANCES IN THE PHYSICAL SCIENCES], 1972, 106, No 4, p 577.

6. Kirichenko A.Ya., "Vozbuzhdeniye periodicheskoy struktury elektronnym 'zaychikom'" ["The Excitation of a Periodic Structure with an Electron 'Wave Crest'"], DAN USSR [REPORTS OF THE UKRAINIAN ACADEMY OF SCIENCES], Series A, "Fiziko-matematicheskiye i tekhnicheskiye nauki" ["Mathematical Physics and the Engineering Sciences"], 1977, No 10, p 926.

7. Kleyen V., "Vvedeniye v elektronika sverkhvysokikh chastot" ["Introduction to SHF Electronics"], Moscow, Sovetskoye Radio Publishers, 1962, Part 1.

8225
CSO:1870

ELECTRONICS AND ELECTRICAL ENGINEERING

UDC 621.396.669

POSTDETECTOR STORAGE IN SIGNAL DETECTION CHANNELS

Kiev IVUZ RADIOELEKTRONIKA in Russian Vol 21 No 11, Nov 78 pp 114-118

[Article by Yu.L. Mazor, manuscript received following revision 3 March, 1978]

[Text] The noise immunity of a typical signal detection channel with power and logic types of postdetector storage for the case of the reception of a weak radio or noise pulse against a background of steady-state noise. Quantitative estimates of the efficiency of the systems considered are derived.

Postdetector storage in a typical detection channel (preselector--detector--low pass filter--threshold gate) can be realized both ahead of and after the threshold gate. A block diagram of a detector with prethreshold (power) storage is shown in Figure 1a, and with postdetector (logic) storage, in Figure 1b. The latter has the advantage that the storage is carried out with the minimum possible volume of information: when the threshold is exceeded, standard pulses are summed.

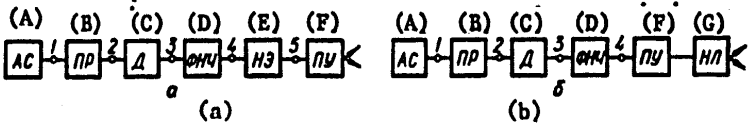

Fiugre 1. Block diagrams of a typical detection channel with power storage (a) and with logic storage (b).

Key: A. AS [antenna system];
B. PR [preselector];
C. D [detector];
D. FNCh [low pass filter];
E. NE [power type storage device];
F. PU [threshold gate];
g. NL [logic type storage device].

The noise immunity of detectors with storage was treated in [1, 2, 3] as applied to the reception of a pulse train; in this case, the optimum number of pulses is determined by working from the minimum requisite power of the pulse train. In a number of detection problems (for example, in the case of passive radar), another formulation is of interest: finding the gain in the noise immunity of a system with storage as a function of the number of storage cycles, from which both the optimal as well as the minimum possible (effective) number of storage pulses can be determined. As far as is known, no comparative assessment of the noise immunity of typical detector channels with power and logic storage has been made in this formulation.

Working from this, given below is a comparative analysis of the noise immunity of these systems in probability terms when detecting weak signals, where it is expedient to use and there is the possibility of reception with storage. The case of the reception of a radio pulse or a noise pulse against a background of steady-state noise is studied.

We shall consider a channel with power storage. We shall make the following assumptions: PR is an ideal bandpass filter with a passband of Δf; D is a bilateral square-law detector; FNCh is an ideal integrator with a switching interval of T. As was shown in [4], for sufficiently weak signals, $\gamma << 1$, and for a rather large product

$$\Delta f T >> 1$$

the signal to noise ratio at the output of the low pass filter is

$$(s/n)_4 = (c/n)_4 = \sqrt{\Delta f T}\gamma,$$

where γ is the ratio of the signal power to the interference power at the output of the preselector.

Following the storage device, in which N-tuple addition is accomplished with a time shift equal to the apriori known period of the signal repetition, assuming constancy of the amplitude of the pulses within the limits of the storage time:

$$(s/n)_5 = (c/n)_5 = \sqrt{N}\,(c/n)_4. \tag{1}$$

Assuming the distribution at the input to the threshold gate to be normal, one can find the correct detection probability (VPO) of a channel with a power type storage device:

$$P_{\text{no m}} = \Phi[\sqrt{N\Delta f T}\,\gamma - \arg\Phi(1 - P_{\text{ml}})], \tag{2}$$

where the probability integral is $\Phi(Z) = \frac{1}{\sqrt{2\pi}}\int_0^z e^{-\frac{x^2}{2}}dx,$

$P_{лт}$ [P_{fa}] is a specified false alarm probability (VLT).

From this, for a detector with power type storage with specified false alarm and correct detectio probabilities:

$$\gamma_{нэ} = \frac{\arg\Phi(P_{по\,нэ}) + \arg\Phi(1 - P_{лт})}{\sqrt{N\Delta f T}}. \qquad (3)$$

By working from formulas (2) and (3), an expression can be derived for the gain in the correct detection probability of a channel with power storage as compared to a similar detector without storage for the case of equal ratios of γ and the false alarm probability:

$$B_{нэ} = \left| \frac{P_{по\,нэ}}{P_{по}} \right|_{\substack{P_{лт}=\text{const} \\ \gamma=\text{const}}} = \frac{\Phi[\sqrt{N\Delta f T}\,\gamma - \arg\Phi(1 - P_{лт})]}{\Phi[\sqrt{\Delta f T}\,\gamma - \arg\Phi(1 - P_{лт})]}, \qquad (4)$$

[$B_{нэ}$ = $B_{\text{power storage}}$], as well as an expression for the gain with respect to the threshold ratios for the same correct detection and false alarm probabilities in the same comparison circuit:

$$Q_{нэ} = \left| \frac{\gamma}{\gamma_{нэ}} \right|_{\substack{P_{по}=\text{const} \\ P_{лт}=\text{const}}} = \sqrt{N}. \qquad (5)$$

The first approach (4) is of interest in working with an object at a constant distance, and the second (5) is of interest when working with a moving signal source.

The characteristics of the advantages gained, $B_{пэ}$ and $Q_{пэ}$, as a function of the number of storage cycles N for various va[illegible]s of the falso alarm probability are shown in Figure 2. When calculatin[illegible] $B_{пэ}$ for each false alarm probability using formula (3), those values of [illegible]re used which at N = 5 provide for a correct detection probability for the case of power storage of 0.9.

We shall consider the noise immunity of a detector with postdetector storage, which performs a "no less than M of N" logic operation, where M is the number of storage cycles where the threshold is exceeded. In this case, we shall assume the assumptions made above are still in force. In the special case of M = N, in a channel with logic storage:

$$P_{лт\,нэ} = P_{лт}^{N}, \qquad (6)$$

$$P_{по\,нэ} = P_{по}^{N} = \{\Phi[\sqrt{\Delta f T}\,\gamma - \arg\Phi(1 - P_{лт})]\}^{N}, \qquad (7)$$

[лт = false alarm; нл = logic storage; п0 = correct detection], where P_{cd} and P_{fa} are the correct detection and false alarm probabilities in a detector without storage. As can be seen from expression (6), $P_{f.a.l.s.} < P_{fa}$, by virtue of which the threshold can be lowered in the detection channel and a gain obtained in the correct detection probability. Thus, the gain in the correct detection probability with respect to a channel without storage, for the case of the same false alarm probabilities and a specified γ:

$$B_{нл} = \left|\frac{P_{п0\,нл}}{P_{п0}}\right|_{\substack{P_{лт}=\text{const},\\ \gamma=\text{const}.}} = \frac{\{\Phi[\sqrt{\Delta fT}\,\gamma - \arg\Phi(1-\sqrt[N]{P_{лт}})]\}^N}{\Phi[\sqrt{\Delta fT}\,\gamma - \arg\Phi(1-P_{лт})]}. \tag{8}$$

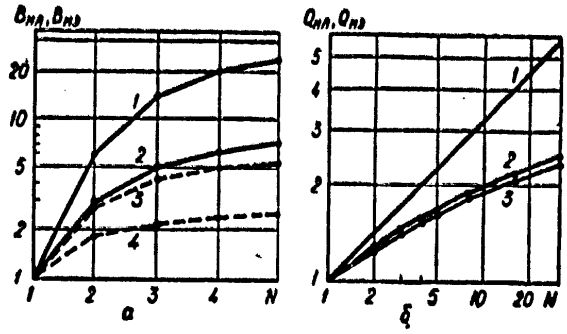

Figure 2. The gain characteristics when $P_{п0нэ}$ [P, correct detection, power storage = P_{cdps}] (N = 5) = $P_{п0нл}$ [P, correct detection, logic storage = P_{cdls}] (N = 5) = 0.9: a. In the correct detection probability, with power storage:

1. $P_{fa} = 10^{-5}$;
2. $P_{fa} = 10^{-3}$;

With logic storage:

3. $P_{fa} = 10^{-5}$;
4. $P_{fa} = 10^{-3}$;

b. In threshold ratios:

1. With power storage;
2. With logic storage, $P_{fa} = 10^{-5}$;
3. With logic storage, $P_{fa} = 10^{-3}$.

[нл = logic storage; нэ = power storage].

An expression can be derived from formula (7) for the ratio γ of a detector with logic storage for specified correct detection and false alarm probabilities:

$$\gamma_{\text{лз}} = \frac{\arg\Phi(\sqrt[N]{P_{\text{п0 лз}}}) + \arg\Phi(1 - \sqrt[N]{P_{\text{лт}}})}{\sqrt{\Delta fT}}, \tag{9}$$

[$\gamma_{\text{нн}} = \gamma$, logic storage], from which the gain in the threshold ratios as compared to a channel without storage for the case of the same correct detection and false alarm probabilities is:

$$Q_{\text{лз}} = \left|\frac{\gamma}{\gamma_{\text{лз}}}\right|_{\substack{P_{\text{п0}}=\text{const}, \\ P_{\text{лт}}=\text{const}}} = \frac{\arg\Phi(P_{\text{п0}}) + \arg\Phi(1 - P_{\text{лт}})}{\arg\Phi(\sqrt[N]{P_{\text{п0}}}) + \arg\Phi(1 - \sqrt[N]{P_{\text{лт}}})}. \tag{10}$$

The gains B_{1s} and Q_{1s} are shown in Figure 2 as a function of the number of storage cycles N for different values of the false alarm probability. The calculation of the ratios γ for the B_{1s} (N) characteristics, which when N = 5 provide for a value of $P_{cd1s} = 0.9$, was carried out using formula (9).

In the general case M ≠ N, on the basis of the theorem concerning the repitition of trials of the false alarm and correct detection probabilities in a channel with logic storage:

$$P_{\text{лт лз}} = \sum_{i=0}^{N-M} C_N^{M+i} P_{\text{лт}}^{M+i} (1 - P_{\text{лт}})^{N-(M+i)}, \tag{11}$$

$$P_{\text{п0 лз}} = \sum_{i=0}^{N-M} C_N^{M+i} \{\Phi[\sqrt{\Delta fT}\,\gamma - \arg\Phi(1 - P_{\text{лт}})]\}^{M+i} \times$$
$$\times \{1 - \Phi[\sqrt{\Delta fT}\,\gamma - \arg\Phi(1 - P_{\text{лт}})]\}^{N-(M+i)}, \tag{12}$$

Where P_{fa} is the false alarm probability in a detector without storage; C_N^M is the number of combinations of N with respect to M.

The gain in the correct detection probability over that of a channel without storage, for the case of same false alarm probabilities and specified ratios of γ, amounts to:

$$B_{\text{лз}} = \left|\frac{P_{\text{п0 лз}}}{P_{\text{п0}}}\right|_{\substack{P_{\text{лт}}=\text{const}, \\ \gamma=\text{const}}} = \left(\sum_{i=0}^{N-M} C_N^{M+i} \{\Phi[\sqrt{\Delta fT}\,\gamma - \arg\Phi(1 - P_{\text{лт0}})]\}^{M+i} \times \right.$$
$$\left. \times \{1 - \Phi[\sqrt{\Delta fT}\,\gamma - \arg\Phi(1 - P_{\text{лт0}})]\}^{N-(M+i)}\right) / \Phi[\sqrt{\Delta fT}\,\gamma - \arg\Phi(1 - P_{\text{лт}})], \tag{13}$$

where $P_{\text{лт0}}$ is the false alarm probability which can be found from the equation

$$\sum_{i=0}^{N-M} C_N^{M+i} P_{\text{лт0}}^{M+i} (1 - P_{\text{лт0}})^{N-(M+i)} = P_{\text{лт}}. \tag{14}$$

The gain in the threshold ratios, Q_{1s}, as compared to a channel without storage, for the case of the same correct detection and false alarm probabilities, can be computed from the family of detection characteristics (12), in which the value of the false alarm probability equal to $P_{ЛТО}$ (14) is substituted.

The gains V_{1s} and Q_{1s} are shown in Figure 3 as a function of the number of storage cycles where the threshold is exceeded, M, for various values of the parameters.

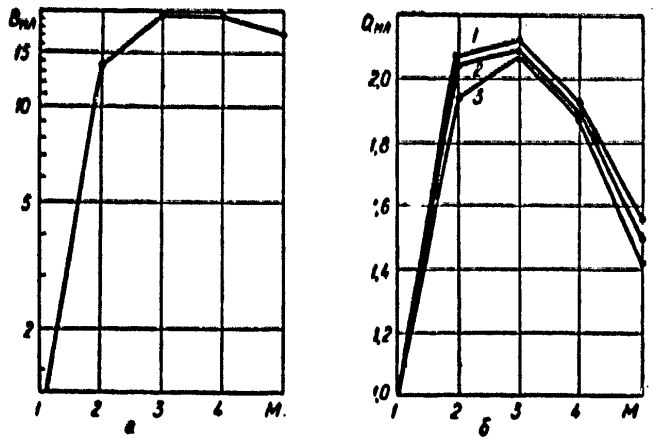

Figure 3. The gain characteristics for the case of storage with "no less than M of N" logic where N = 5; $\Delta fP = 10^5$;

a. In the correct detection probability where $\gamma = 0.01$; $P_{fa} = 10^{-6}$;

b. In threshold ratios γ when $P_{cd} = 0.9$;

1. $P_{fa} = 10^{-4}$;
2. $P_{fa} = 10^{-3}$;
3. $P_{fa} = 10^{-2}$.

Thus, a comparative assessment of the noise immunity of typical detection channels with storage permits the following conclusions:

--Typical detection channels with power storage (Figure 1a) have a substantial noise immunity advantage over channels with logic storage (Figure 1b);

--The analytical expressions derived for the gain in the noise immunity, B_{ps} (N), B_{1s} (N), Q_{ps} (N) and Q_{1s} (N) and the graphical functions (Figures 2 and 3) can be used to determine the optimum number of storage cycles;

--A characteristic feature of the curves for Q_{1s} (M) and B_{1s} (M) when N = const. (Figure 3) is the presence of a maximum at the optimum ratio of M to N.

BIBLIOGRAPHY

1. Gutkin L.S., "Teoriya optimal'nykh metodov radiopriyema pri flyuktuatsionnykh pomekhakh" ["The Theory of Optimal Radio Reception Methods for the Case of Fluctuating Noise"], Moscow, Sovetskoye Radio Publishers, 1972.

2. "Voprosy statisticheskoy teorii radiolokatsii" ["Questions in the Statistical Theory of Radar"], Edited by G.P. Tartakovskiy, Moscow, Sovetskoye Radio Publishers, 1963.

3. Lezin Yu.S., "Optimal'nyye fil'try i nakopiteli impul'snykh signalov" ["Optimal Filters and Storage Devices for Pulse Signals"], Moscow, Sovetskoye Radio Publishers, 1969.

4. Gatkin N.G., Geranin V.A., Karnovskiy M.I., Krasnyy L.G., "Pomekhoustoychivost' tipovogo trakta obnaruzheniya signalov" ["The Noise Immunity of a Conventional Signal Detection Channel"], Kiev, Tekhnika Publishers, 1971.

8225
CSO:1870

ELECTRONICS AND ELECTRICAL ENGINEERING

UDC 621.372.54.037.372

PROCESSING A SIGNAL WITH A RANDOM DELAY USING A DIGITAL MATCHED FILTER

Kiev IVUZ RADIOELEKTRONIKA in Russian Vol 21 No 11, Nov 78 pp 123-124

[Article by I.P. Knyshev, manuscript received 18 November, 1977]

[Text] A received signal, which is processed in a digital matched filter (TsSF), has a certain delay. This delay is proportional to the range to the target in the case of a radar system, or to the spacing between the transmitter and the receiver in the case of an information transmission system.

The received signal can be written as:

$$x'(nT) = x(nT + t_{зап}),$$

where x(nT) is the transmitted signal; $t_{зап}$ [t_{del}] is the delay time.

The size of t_{del} can be expressed in terms of the quantization interval P as

$$t_{del} = N_0 T + \xi T ,$$

where N_0 is an integer and $|\xi| \leq 0.5$.

As shown in [1], a delay by an integer number of quantization intervals does not influence the shape of the output signal of a digital matched filter, but rather leads to a shift in this signal by the same time interval $N_0 T$.

It is also indicated in this same paper that a delay by a time less than the quantization interval leads to mismatching of the pulse response of the digital matched filter and a decrease in its maximum.

Thus, the delay ξT causes a degradation of the output signal to noise ratio. The amount of the loss in the signal to noise ratio can be found from the reduction in the amplitude of the digital matched filter response:

$$\eta(\xi) = \frac{y'(0)}{y(0)}, \qquad (1)$$

where $y'(0) = \sum_{k=0}^{N} x(kT + \xi T)\, x(mT - kT) = R(\xi T)$ is the digital matched filter response to the delayed signal, where m = 0.

$$y(0) = \sum_{k=0}^{N} x(kT)\, x(mT - kT) = R(0)$$

is the response of the digital matched filter to a signal without a delay, where m = 0.

Considering the fact that y(0) is the autocorrelation function of the signal x(nT), and y'(0) can be treated as a shifted autocorrelation function, expression (1) can be represented as:

$$\eta(\xi) = \frac{R(\xi T)}{R(0)}. \tag{2}$$

Expression (2) permits finding the losses as a function of the delay or as a function of the system parameters, based on the known autocorrelation function.

Thus, for a signal which is the discrete analog of a linear FM signal:

$$x(nT) = \cos\left[\frac{W(nT)^2}{2T_u}\right], \quad 0 \leqslant n \leqslant N, \tag{3}$$

where T_u [T_i] is the signal width and W is the width of the deviation bandwidth, the autocorrelation function has the following form:

$$R(mT) = \frac{\sin\left(\frac{WmT}{2T_u} NT\right)}{\sin\left(\frac{WmT}{2T_u} T\right)} \cos\left\{\frac{WmT}{2T_u}\left[mT + (N-1)T\right]\right\}. \tag{4}$$

If it is assumed that losses are maximal at the maximum mismatching of the readouts of the signal and the filter response (ξ = 0.5), and also taking into account the relationship N = 2B, $WT_i = 2\pi B$, $P_i = NT$ and expression (4), or the size of the losses (2) can be represented as:

$$\eta_{max} \simeq \eta_{max} = \frac{1}{\pi} \sin\left(\frac{\pi}{l}\right). \tag{5}$$

The graph of the maximum losses as a function of the digitization interval is shown in Figure 1, where 1 is the maximum losses ν_{max}, and 2 are the average losses ν_{avg}. Figure 1 attests to the fact that to obtain low losses, it is necessary to select a rather high digitization frequency. The value of this frequency should be more than twice as high as the upper value of the frequency deviation ($\omega_{discr} \geq W$).

The delay ξT can be treated as a continuous random quantity with a zero average value and a probability density $p(\xi) = 1/T$. Consequently, the size of losses is also a random quantity. The average value of this quantity can be defined as [2]:

$$\eta_{avg} = \eta_{cp} = \int_{-0.5T}^{0.5T} \eta(\xi)\, p(\xi)\, d\xi T = \frac{1}{TR(0)} \int_{-0.5T}^{0.5T} R(\xi T)\, d\xi T. \tag{6}$$

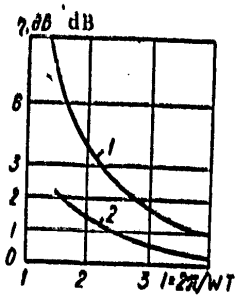

Figure 1.

Expression (6) permits the determination of the average value of the losses in a system or the selection of the values of the parameters based on the known autocorrelation function.

Thus, for signal (3), which has the autocorrelation function (4), the average size of the losses is equal to

$$\eta_{avg} \approx \eta_{cp} \approx 1 - \frac{0{,}5\pi^2}{q^2} + \frac{0{,}03125\pi^4}{3q^4}. \qquad (7)$$

Shown in Figure 1 (curve 2) is the size of the average losses (7) as a function of the quantization interval. As was to be expected, the size of average losses is substantially less than the maximal losses.

Depending on the specific requirements placed on a system, the size of the digitization interval can be chosen based on the maximal or the average losses.

Expression (2) or (6) can serve as a criterion for the choice of a signal which provides a minimum of losses from the random time of signal arrival. The optimal signal in this case will be one with a minimal change in the value of the autocorrelation function in the range [-0.5 -- +0.5]T.

Where necessary, in accordance with the general procedure of [2], other characteristics of the random size of the losses can also be found (the dispersion, probability density distribution).

BIBLIOGRAPHY

1. Gol'denberg L.M., Levchuk Yu.P., Polyak M.N., "Tsifrovyye fil'try" ["Digital Filters"], Moscow, Svyaz' Publishers, 1974.

2. Levin B.R., "Teoreticheskiye osnovy statisticheskoy radiotekhniki" ["The Theoretical Principles of Statistical Radio Engineering"], Moscow, Sovetskoye Radio Publishers, 1974, 1.

8225
CSO:1870

ELECTRONICS AND ELECTRICAL ENGINEERING

UDC 621.391.8

THE NOISE IMMUNITY OF THE OPTIMUM DETECTION OF FLUCTUATING SIGNALS IN NOISE OF AN UNKNOWN LEVEL

Kiev IVUZ RADIOELEKTRONIKA in Russian Vol 21 No 11, Nov 78 pp 124-127

[Article by K.K. Vasil'yev, manuscript received following revision 10 November 1977]

[Text] The problem of the incoherent detection of packets of pulse signals against a background of normal noise with an unknown dispersion is frequently encountered in the design of radio systems. In many cases, this problem is effectively solved using a contrast procedure, which consists in processing two independent samples from the envelope of the input process. One of them, $\{x_{si}\}_{i=1}^{N}$, can contain the useful signal, while the second, $\{x_{0i}\}_{i=1}^{M}$ is a graded teaching sample in the region of the interference [1].

The application of the maximum plausibility method [2] and the empirical theory of [3] for the case of samples of equal volume (M = N), has permitted the finding of the most uniformly powerful empirical rule (RNMN) for signal detection [2, 3].

The results obtained earlier can be extended to the case considered here for samples of different volumes. In this case, the RNMN rule for the detection of a signal with a random amplitude is written in the following form: there is a signal if:

$$y = \lambda_s/\lambda_0 > \gamma, \tag{1}$$

where $\lambda_s = \sum_{i=1}^{N} x_{si}^2$; $\lambda_0 = \sum_{i=1}^{M} x_{0i}^2$; ; γ is a constant defined by the specified false alarm probability.

The noise immunity of the resulting optimal procedure (1) is analyzed in this paper as a function of the number of signal positions N and the number of reference interference readouts M. In this case, it is assumed that the distribution density of the probabilities for the readouts $\{x_{si}\}$ and $\{x_{0i}\}$ can be represented by the following expressions where the useful signal is present:

$$w(\vec{x}_s) = \prod_{i=1}^{N} w(x_{si}) \text{ и } w(\vec{x}_0) = \prod_{i=1}^{M} w(x_{0i}),$$

where $w(x_{si}) = [x_{si}/(1+S)\sigma^2] \exp[-x_{si}^2/2\sigma^2(1+S)]$ is the law governing the distribution of the probabilities of the envelope of the sum of the normal noise and a signal with random amplitude; S is the ratio of the signal power to the noise dispersion σ^2; $w(x_{0i}) = (x_{0i}/\sigma^2)\exp(-x_{0i}^2/2\sigma^2)$.

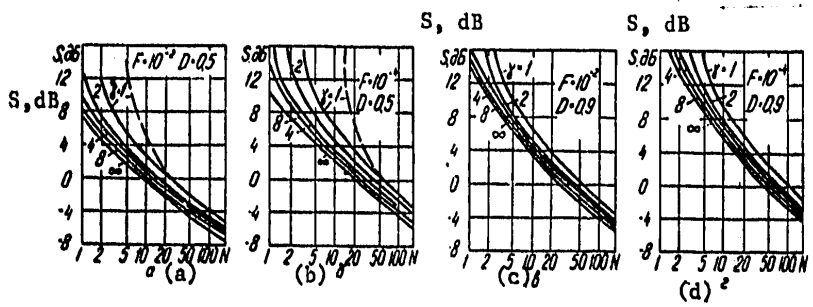

Figure 1.

To find the power function for rule (1), we note that the squares x_{si}^2 and x_{0i}^2 of the readouts in the regions of the signal and interference have an exponential distribution. For this reason, the statistics λ_s and γ_0 obey a gamma distribution, and consequently, the random quantity $z = y/(1+S)$ has a Fisher z-distribution: $w(z) = \Gamma(M+N)z^{N-1}/\Gamma(M)\Gamma(N) \cdot (1+z)^{M+N}$, where $\Gamma(\cdot)$ is the gamma function of [5].

In this case, the detection algorithm power function for (1) can be expressed in terms of a complete B(N, M) and an incomplete $B_q(N, M)$ beta function [4] in the following manner:

$$\beta = 1 - B_q(N, M)/B(N, M),$$

where $q = \theta/(1+\theta)$; $\theta = \gamma/(1+S)$.

For calculations on a computer, it is convenient to represent this relationship in the following form:

$$\beta = \frac{1}{(1+\theta)^{M+N-1}} \sum_{i=0}^{N-1} \theta^i C_{M+N-1}^i.$$

We shall determine the level of the threshold signal S from the condition $\beta(s, \gamma) = D$, where D is a specified correct detection probability. In this case, we find the constant γ from the specified false alarm probability $\beta(s = 0, \gamma) = F$.

The threshold signal levels are shown in Figure 1 as a function of the number of analyzed signal positions N for various ratios of $\nu = M/N$ sample volumes in the regions of the noise and signal when $F = 10^{-2}$ and 10^{-4}, and $D = 0.5$ and 0.9.

As can be seen from the Figures, the threshold signal level decreases with an increase in the relative number of interference readouts ν. When $\nu \to \infty$, the effectiveness of the algorithm considered here coincides with the case where the optimal procedure $\lambda_s \gtrless \gamma$ is used for the detection of fluctuating signals in noise of a known power. A decrease in the volume of the sample in the interference region leads to losses in the threshold signal, which are caused by the apriori unknown noise level. In this case, the amount of the loss with respect to the case of a known dispersion increases both with a decrease in the specified false alarm probability and in the case of a shortening of the length of the pulse packet.

To compute the effectiveness for a large number of analyzed signal positions N, it is expedient to make use of the following approximate formula.

$$\beta \cong 0{,}5 - \Phi_0\left(\sqrt{N}\,\frac{v\theta - 1}{\sqrt{v\theta^2 + 1}}\right),$$

where $\Phi_0(x) = \frac{1}{\sqrt{2\pi}}\int_0^x e^{-0{,}5u^2}\,du$, which is found for the conditions of a gaussian distribution of the statistics $\gamma_s - \gamma\lambda_0$.

In this case, the simplest expression is successfully derived for the threshold signal level if $D = 0.5$. Then $S = S = a + a\sqrt{1 + (v+1)/a}$, where $a = x_F^2/(M - x_F^2)$; x_F is the normal distribution quantile at the 1-F level (Table 1).

Table 1

F	10^{-1}	10^{-2}	10^{-3}	10^{-4}	10^{-5}	10^{-6}	10^{-8}	10^{-10}
x_F	1,28	2,33	3,09	3,72	4,25	4,75	5,62	6,38

Analysis shows that the relationships given here approximate the S(N) function considered with an error of less than 5%, if $N > 50$. By way of illustration, characteristic curves (the dashed line), computed taking the approximate formulas into account, are shown in Figures 1a and 1b.

We shall make use of the criterion of the asymptotic relative effectiveness (AOE) of algorithm (1) and the optimal signal detection rule for the case of completely known interference parameters to compare the signal processing procedures when $N \to \infty$. In this case, the the AOE can be computed from the following formula [1]:

$$\rho = \lim_{\substack{N\to\infty \\ S\to 0}} \frac{N_0}{N} = \lim_{\substack{N\to\infty \\ S\to 0}} \frac{[\partial m_1(y)/\partial S]^2}{N\sigma_y^2},$$

where N_0 and N are the number of analyzed signal positions for the optimal algorithm and the algorithm considered here respectively; $m_1(y)$ is the mathematical mean value of the statistic y when the useful signal is present; σ_y^2 is the dispersion of y when $S = 0$.

By calculating:

$$m_1(y) = \frac{N(1+S)}{M-1} \text{ и } \sigma_y^2 = \frac{N(M+N-1)}{(M-1)^2(M-2)},$$

taking into account the well known expressions for the moments of the Fisher z-distribution [4], it is not difficult to find the following formula for the size of the AOE;

$$\rho = \frac{M}{M+N}.$$

The derived expression provides the possibility of rather simply determining the requisite increase in the length of a pulse packet as a function of the number of reference readouts M, which allow for the obtaining of additional information on the interference dispersion. As calculations show, the asymptotic formula found here approximates the precise relationships with an error of less than 5%, if $N > 500$.

Thus, as a result of the analysis made here, precise and approximate formulas were derived which are needed to estimate the noise immunity of optimal detection of packets of fluctuating signals in noise with an unknown dispersion.

BIBLIOGRAPHY

1. Levin B.R., "Teoreticheskiye osnovy statisticheskoy radiotekhniki" ["The Theoretical Principles of Statistical Radio Engineering"], Moscow, Sovetskoye Radio Publishers, 1976, Book 3.

2. Prokof'yev V.N., "Obnaruzheniye pachki signalov s neizvestnymi parametrami v shumakh neizvestnogo urovnya" ["The Detection of a Signal Packet with Unknown Parameters in Noise of an Unknown Level"], IZV. VUZOV - RADIOELEKTRONIKA [PROCEEDINGS OF THE HIGHER EDUCATIONAL INSTITUTES, RADIO ELECTRONICS], 1972, 15, No 10, p 1,234.

3. Prokof'yev V.N., "K zadache obnaurzheniya signalov v shumakh neizvestnogo urovnya" ["On the Problem of Signal Detection in Noise of an Unknown Level"] RADIOTEKHNIKA I ELEKTRONIKA, 1969, 14, No 10, p 1,895.

4. Kramer G., "Matematicheskiye metody statistiki" ["Mathematical Methods of Statistics"], Moscow, Mir Publishers, 1975.

5. Gradshteyn, I.S., Ryzhik I.M., "Tablitsy integralov, summ, ryadov, i proizvedeniy" ["Tables of Integrals, Sums, Series and Products"], Moscow, Nauka Publishers, 1971.

8225
CSO:1870

ELECTRONICS AND ELECTRICAL ENGINEERING

UDC 621.396.96

THE REFLECTION OF A QUASICONTINUOUS SIGNAL FROM THE SURFACE OF THE EARTH AT SMALL GRAZING ANGLES

Kiev IVUZ RADIOELEKTRONIKA in Russian Vol 21 No 11, Nov 78 pp 133-135

[Article by L.F. Vasilevich and N.A. Vinogradov, manuscript received 14 December, 1977]

[Text] In studying groundreturns, a statistically rough surface is usually employed as the model of the reflecting area [1]. In this paper, this surface is treated as a filter with randomly changing characteristics. Such an approach permits the use of the well developed tools of parametric systems theory.

We shall write the reflected signal in the form of the sum of the returns from the elemental areas:

$$y(t)=\sum_{i=1}^{N}\frac{K(t,t_i)}{\Delta l}Q(\varphi_i)\,x(t-t_i)\,\Delta l;\ \Delta l=\frac{2\Delta D}{cN},$$

where $K(t, t_i)$ is the reflection factor of the i-th reflecting area; ΔD is thesize of an elemental area, within the bounds of which one can consider the reflection characteristic to be constant; c is the propagation velocity of the radio waves; $Q(\phi_i)$ is the shading function of [1]: $Q(\phi_i)=Q\left(\arcsin\frac{2h_a}{d}\right)$: ϕ_i is the grazing angle; h_a is the height of the antenna.

It is usually assumed that the signal reflected from an elemental reflector does not influence other signals. It was noted in [2] that the setting of conditions which define the mutual influences of the elemental reflectors does not produce any marked change in the results.

Taking this into account, one can go to the limit where $\Delta t \to 0$ and $N \to \infty$:

$$y(t)=\int_{\tau_{min}}^{\tau_{max}}Q(\tau)\,k(t,\tau)\,x(t-\tau)\,d\tau,$$

where τ_{min} and τ_{max} are the delay limts of the reflected signals; $k(t, \tau) = -\lim_{\Delta t\to\tau}\frac{K(t,t_i)}{\Delta l}$ is the pulse characteristic of the reflection of the surface segment.

If a pulsed signal with an amplitude A and a period T_π [T_p] is used as the sounding signal,

$$x(t) = \sum_{m=1}^{M} A(t - mT_\pi) \exp[-j2\pi f(t - mT_\pi)],$$

then the reflected signal assumes the form:

$$y(t) = \int_{\tau_{min}}^{\tau_{max}} \sum_{m=1}^{M} Q(\tau) k(t - mT_\pi, \tau) A(t - mT_\pi - \tau) \exp[-j2\pi f(t - mT_\pi - \tau)] d\tau.$$

Let another set of elemental reflectors be located at a certain distance D_2. The signal reflected from it will be:

$$y(t) = \int_{\tau_{min}}^{\tau_{max}} Q(\tau) k(t - v, \tau) x(t - v - \tau) d\tau,$$

where

$$v = \frac{2D_2}{c}.$$

When computing the correlation function (KF) of the reflected signal, it is necessary to consider the statistical characteristics of the roughness of the reflecting surface. Taking this into account, we write the correlation function in the form:

$$R(t, v) = \int_{-\infty}^{\infty}\int y(t, h_1) y(t - v, h_2) W_2(h_1, h_2) dh_1 dh_2,$$

where $W_2(h_1, h_2)$ is the two-dimensional law for the distribution of the heights.

The assumption that the distribution of the heights of the points of the reflecting surface is close to a normal distribution is substantiated in [1, 3, 4]. Considering $W_2(h_1, h_2)$ to be normal, following several cumbersome transformations, the correlation function can be reduced to the form:

$$R(t, v) = k_1 \int_{-\infty}^{\infty}\int y(t, h_1) y(t - v, h_2) \exp\left\{-\left(\frac{4\pi}{\lambda} \sigma_h \cos\varphi\right)^2 [1 - \rho(h)]\right\} dh_1 dh_2,$$

where σ_h is the SKO [expansion unknown] of the surface heights; ϕ is the grazing angle; λ is the wavelength; $\rho(h)$ is the correlation function of the surface heights; and k_1 is a proportionality factor.

It is noted in [3] that an exponential correlation function of the heights is the one most frequenctly chosen, since when it is used, the dependence of the reflection characteristics on frequency is taken into account. However, it was demonstrated in [2] that this correlation function corresponds to a signal which does not posses the property of regularity at the origin of the coordinates, and for this reason, cannot be used for estimating the surface properties at this point. It should be noted that the experimentally obtained correlation functions likewise differ from the exponential ones close to the origin of the coordinates. This particular feature must be considered when estimating the parameters of the reflected signal.

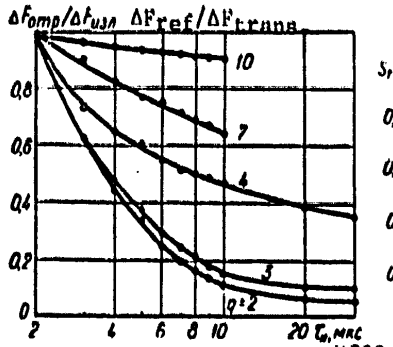

Рис. 1.

Figure 1.

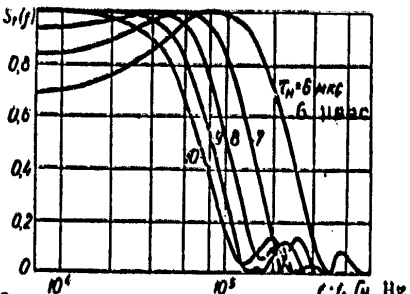

Рис. 2.

Figure 2.

It is sometimes assumed that the signal reflected from the ground is a steady-state process, however, it was noted in [4] that the nonsteady-state nature of the background plays a substantial part.

We shall employ a locally steady-state process, which yields good results when studying actual phenomena, as a model here. The correlation function of such a process has the form:

$$R(t, v) = R_1(t) R_2(v) = R_1\left(\frac{t_1 + t_2}{2}\right) R_2(t_1 - t_2),$$

where $R_1(t) = R_1\left(\frac{t_1 + t_2}{2}\right)$ is a multiplying factor proportional to the nonsteady-state dispersion; $R_2(v) = R_2(t_1 - t_2)$ is the correlation function of the steady-state process.

When irradiating a section of the ground surface, there occurs averaging of the reflected signal in both space and time.

The spectrum of the signal which is averaged in space within the limits of the resolvable area can be treated as either instantaneous or of short duration [5].

$$S_u(f, v) = \int_t^{t+\tau} R(t, v) \exp(-j2\pi f t)\, dt.$$

Within the limits of the width of the directional pattern with respect to the elevation angle, for the case of grazing propagation, the pulses of a quasicontinuous signal are reflected immediately from several sections, which are separated from each other by a range $\Delta D = cT_p/2$. Of substantial interest for the signal studied here is the spectrum when averaged over several repitition periods (the current spectrum of [5]):

$$S_\tau(f, \tau_u) = \int_0^{\tau_u} S_u(f, v)\, dv, \qquad (1)$$

where τ_H is the storage time.

To estimate the shape and width of the current spectrum, experimental studies were carried out and calculations were performed on a computer. The experimental results are shown in Figure 1, where $f_0 = 10^{10}$ Hz, $\tau_i = 1$ μsec, $\psi_0 = 2°$, $q = T_{rep}/\tau_i$, while the calculations are shown in Figure 2, where $f_0 = 10^{10}$ Hz, $T_{rep} = 330$ KHz, $\tau_i = 1$ μsec and $\tau_{corr} = 5$ μsec. Here, $S_T(f, \tau_H) = \text{const.}$, when $|f - f_0| < 10^4$ Hz.

An analysis of the resultant data attests to the rather good agreement of the computed and experimental results.

The limitations of a correlation function in the form of an exponential one were noted above. To specify the results in the expression under the integral sign more precisely for integral (1), an additive regularizing operator was introduced,

$$\omega(\tau, \alpha) = \alpha \int_0^{\infty} (\exp(-/4\pi/f) - 4\pi^2/^2 \exp(-2\pi/f))\, df$$

(α is the regularization parameter of [6]). The operator $\omega(\tau, \alpha)$ was computed by a variation procedure. It should be noted that without the introduction of the operator $\omega(\tau, \alpha)$, strong oscillations of the spectrum appear at frequencies which are multiples of the repetition rate.

Thus, the calculations performed here allow for the following conclusions:

1) The spectrum of a quasicontinuous signal reflected from a section of the earth's surface, contains a marked coherent component, and in terms of its characteristics, approximates the spectrum of a reflected continuous signal;

2) This effect is manifest at small grazing angles of the beam, and apparently, is related to a reduction in the pulse volume of the number of reflectors, which make the most substantial contrications to the resulting signal.

BIBLIOGRAPHY

1. Bass F.G., Fuks I.M., "Rasseyaniye voln na statisticheski nerovnoy poverkhnosti" ["Wave Scattering at a Statistically Uneven Surface"], Moscow, Nauka Publishers, 1972.

2. Zubkovich S.G., "Statisticheskiye kharakteristiki radiosignalov, otrazhennykh ot zemnoy poverkhnosti" ["The Statistical Characteristics of Radio Signals, Reflected from the Earth's Surface"], Moscow, Sovetskoye Radio Publishers, 1968.

3. Moore R.K., "Radar Return from the Ground", THE BULLETIN OF ENG., Lawrence Kansas, 1969, No 59.

4. Sokolov A.V., "Metody modelirovaniya radiolokatsionnykh tseley (obzor)" ["Methods of Modeling Radar Targets (Review)"], ZARUBEZHNAYA RADIOELEKTRONIKA [FOREIGN RADIOELECTRONICS], 1974, No 6.

5. Kharkevich A.A., "Spektry i analiz" ["Spectra and Analysis"], Moscow, Fizmatgiz Publishers, 1962.

6. Tikhonov A.N., Arsenin A.Ya., "Metody resheniya nekorrektnykh zadach" ["Methods of Solving Improper Problems"], Moscow, Nauka Publishers, 1974.

8225
CSO:1870

ELECTRONICS AND ELECTRICAL ENGINEERING

UDC 621.373.42.001.57

MODELING THE PROCESSES IN A SELF-OSCILLATING SYSTEM WHICH IS ACTED UPON BY A REFLECTED DELAYING SIGNAL

Kiev IVUZ RADIOELEKTRONIKA in Russian Vol 21 No 11, Nov 78 pp 137-139

[Article by V.G. Lysenko and A.R. Mileslavskiy, manuscript received following revision 17 April, 1978]

[Text] The problem of studying a self-oscillating system, which is acted upon by a reflected delaying signal arises in a number of engineering applications [1]. Such systems have been called autodyne systems. Despite the fact that considerable literature has been devoted to autodynes [1 - 4], several questions are far from completely worked out.

Little attention has been devoted in the literature to studying the processes in an autodyne for the case of large levels of external input which are comparable to the self-oscillations. The goal of this paper is to partially fill in this gap. The problem of the behavior of an autodyne system at high reflected signal levels is not only of theoretical, but also of practical interest, since in solving it, one can, in the first place, find the limit of the applicability of linear theory [1 - 3], and secondly, answere the question at which parameters is external synchronization of an autodyne impossible. As was shown in [4], the presence of synchronization leads to a substantial reduction in the doppler component in the spectrum of the output signal of the autodyne, i.e., to a disruption of the operability of the device.

In approximating the static characteristic of an active element with the function $i(u) = S_1u - S_3u^3$, an autodyne system can be described by a nonlinear differential equation with a delaying argument:

$$p^2x(t) - \varepsilon\omega_0[1 - x^2(t)]px(t) + \omega_0^2x(t) = k\delta\omega_0^2x[t - \tau(t)], \quad (1)$$

which when $k = 0$ coincides with Van der Pol's equation. Here p is the differential operator; $x(p) = [3S_3R_y/(S_1R_y - 1)]^{1/2}u(t)$ is the normalized voltage; R_y is the controlling resistance of the generator; $\varepsilon = \delta(S_1R_y - 1)$;

δ and ω_0 are the attenuation and resonant frequency of the tuned circuit; k is the ratio of the amplitude of the external force to the amplitude of the self-oscillations ($k < 1$); $\tau(t)$ is a variable delay due to the relative motion of the autodyne and the objects being studied.

Precise analytical methods of solving equation (1) do not exist, even for small values of k. In this work, equation (1) was studied on an MN-18M analog computer, in accordance with the structural configuration shown in Figure 1, where the dashed line encloses the electronic analog of the self-oscillating system. The remaining part of the circuit, which contains five integrators, seven multipliers and five adders, takes the form of a variable delay block, the parametric transfer function of which has the form [5]:

$$S(p, t) = \frac{19{,}4 - 7{,}63\tau(t)p + \tau^2(t)p^2}{19{,}4 + 7{,}63\tau(t)p + \tau^2(t)p^2} \cdot \frac{54{,}9 - 5{,}94\tau(t)p + \tau^2(t)p^2}{54{,}9 + 5{,}94\tau(t)p + \tau^2(t)p^2}. \quad (2)$$

A linear function of $\tau(t)$ ($d\tau/dt \ll 1$) was used in the modeling, something which corresponds to a uniform relative motion of the autodyne and the object. The delay $\tau(t)$ was placed outside the differential operator sign in (2), something which, as analysis shows, does not lead to substantial errors.

Transfer function (2) provides for the greatest value of the parameter $\omega_0\tau_{max} = 7.44$ at a specified phase error (0.1 rad) as compared to other well known approximations of an ideal delay network [5]. This permits observing the solution of equation (1) in a time segment which is at least equal to one period of the doppler frequency $\Omega = \omega_0 d\tau/dt$.

The operator S(p, t) can be realized by means of two series connected stages which have identical transmission coefficients. The method of implicit functions [6] was employed when selecting each of these coefficients on the analog computer. Operational amplifiers, looped by negative feedback through capacitors with a small capacitance play the part of integrators with a high gain [6] (Figure 1).

The results of the modeling for two levels of the reflected signal, $k = 0.3$ and $k = 0.9$ are shown in Fiugre 3a, b ($\omega_0 = 2\pi$, $\omega_0/\Omega = 100$). A drawback to modeling based on the entire equation (1) is the fact that it is impossible to observe its solution over several periods of the doppler frequency. For this reason, a second modeling stage was carried out, based on truncated eqations found from (1) by conventional methods. We will note that the results of both experiments are in qualitative agreement.

It can be seen from Figure 2a, b that the voltage across the tunded circuit of the autodyne takes the form of an amplitude modulated signal. The frequency of the modulation, and this is extremely important, almost does not change with an increase in the level of the reflected signal k. When $k \leq$ $\leq$ 0.1--0.3, the law governing the modulation is close to a harmonic one.

Thus, it can be assumed that the lineat theory of an autodyne is justified in the given case up to values of $k \leq 0.1$--0.3. With an increase in k, the modulation level increases, approaching 100%, and in this case, the law governing the modulation differes from a sinusoidal one. However, this difference is small and will have practically no effect on the normal functioning of the low frequency processing circuitry.

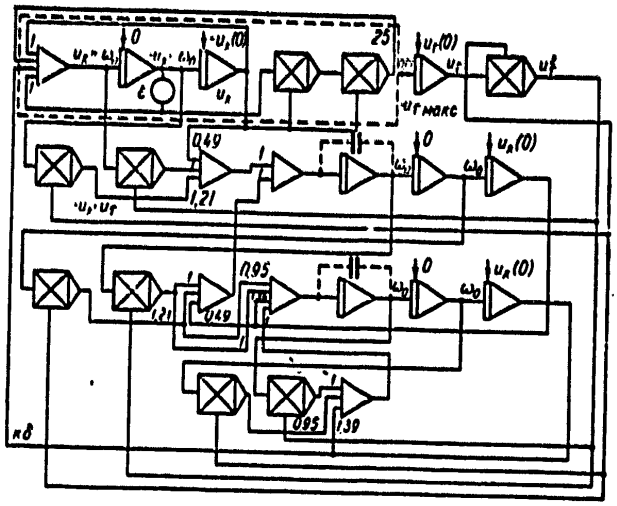

Figure 1.

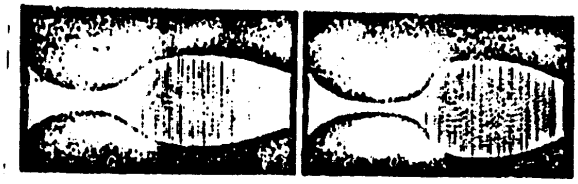

Figure 2.

It follows from the modeling results that even for large levels of the reflected signal (k = 0.9), the system does not go into synchronization. We shall deal with this question in more detail.

We shall establish the relationship between the delay time $\tau(r) = 2r/c$ (r is the distance; c is the speed of light) and the time constant $T_c(r)$,

which characterizes the rate of the processes during synchronization and determines the time for establishing a synchronous mode. We shall make use of the well known formula of [7] to estimate $T_c(r)$:

$$T_c(r) = \frac{1}{\omega_0 \delta \eta}\left(\frac{P_{изл}}{P_{пр}}\right)^{1/2}, \tag{3}$$

where ν is the efficiency of the resonant circuit; $P_{изл}$ is the power radiated by the autodyne; $P_{пр}$ is the power of the received signal. The proportionality factor between them in the near field has the form [1]:

$$\frac{P_{пр}}{P_{изл}} = \frac{\lambda^2 G_a^2 N_0^2}{64\pi^2 r^4}, \tag{4}$$

where λ is the wavelength; G_a is the antenna gain; N_0 is the coefficient which takes into account the losses with reflection from the object being studied, and is usually equal to 0.3--1.

Taking (3) and (4) into account, we obtain

$$\tau(r)/T_c(r) = 0{,}5\,\delta\eta G_a N_0. \tag{5}$$

It can be seen that neither the range r nor the working frequency of the autodyne ω_0 enters directly into (5).

It follows from relationship (5) that if an antenna with a gain of $G_a \ll 1/\delta$ is employed in the autodyne (this is the most widespread case in practice), then $\tau \ll T_c$, and there can be no synchronization in such a system. This is explained by the inertia of the synchronization process itself, and is confirmed, in particular, by the results of analog modeling.

BIBLIOGRAPHY

1. Kogan I.M., "Blizhnyaya radiolokatskiya" ["Near Field Radar"], Moscow, Sovetskoye Radio Publishers, 1973.

2. Bogachev V.M., Lysenko V.G., Smol'skiy S.M., "K teorii avtodinov na inertsionnykh aktivnykh elementakh" ["On the Theory of Autodynes using Inertial Active Elements"], IZV. VUZOV - RADIOELEKTRONIKA [PROCEEDINGS OF THE HIGHER EDUCATIONAL INSTITUTES - RADIO ELECTRONICS], 1976, 19, No 5, p 62.

3. Takayama Y., "Doppler Signal Detection with Negative Resistance Diode Oscillators"], IEEE TRANS., 1973, MTT-21, No 2.

4. Tamarchak D.Ya., Khotuntsev Yu.L., "Povedeniye sinkhronizirovannogo generatora pri vozdeystvii sil'nykh signalov s izmenyayushcheysya chastotoy" ["The Behavior of a Synchronized Oscillator with the Action of Strong Signals having a Changing Frequency"], RADIOTEKHNIKA I ELEKTRONIKA, 1977, 22, No 7.

5. Korn G., Korn T., "Elektronnyye analogovyye i analogovo-tsifrovyye vychislitel'nyye mashiny" ["Electronic Analog and Analog-Digital Computers"], Moscow, Mir Publishers, 1968, Part 2.

6. Urmayev A.S., "Osnovy modelirovaniya na analogovykh vychislitel'nykh mashinakh" ["The Principles of Modeling on Analog Computers"], Moscow, Nauka Publishers, 1974.

7. Adler R., "Issledovaniye yavleniy sinkhronizatsii generatorov" ["An Investigation of Oscillator Synchronization Phenomena"], TIIER, 1973, 61, No 10.

8225
CSO:1870

GEOPHYSICS, ASTRONOMY AND SPACE

UDC 550.831.01

CORPUSCULAR MODEL OF GRAVITATION AND INERTIA

Moscow PRIKLADNAYA GEOFIZIKA in Russian No 87, 1977 pp 92-106

[Article by K.Ye. Veselov]

[Text] The corpuscular model of gravitation and interia described is based on the familiar concepts of Lomonosov and Le Sage regarding the mechanism of gravitational interaction and on inferences from the special theory of relativity. In it is hypothesized the existence in an entire space of particles which travel chaotically at an enormous speed and penetrate all bodies, losing in the process only a very moderate portion of their momentum. Such a space is called a gravitational vacuum. Bodies in a gravitational vacuum, because of mutual screening [4], will be attracted according to the inverse square law. The vacuum will also exert resistance to a change in the state of motion of a body, i.e., will create inertia.

In the corpuscular model is discussed not a formal transition from one inertial system of reference to another, but a transition through accelerated motion, the energy of forces, and modification of the mass of bodies. The corpuscular model of gravitation and inertia explains satisfactorily, quantitatively and qualitatively, three familiar effects of the general theory of relativity, and, in addition, secular and seasonal variations in the length of the terrestrial day and shortening of the year. It can also be enlisted for the purpose of explaining many geological and geophysical effects.

In the corpuscular model the following limitations are imposed on interaction between the vacuum and bodies.

1. Particles in the gravitational vacuum possess a steady state of chaotic motion with a maximum rate of propagation of physical interactions of c. With linear and uniform motion, between the bodies and the gravitational vacuum an exchange of momentum is carried out and on average the condition of dynamic equilibrium is fulfilled. If a single body is at rest or moves through inertia, then the force of hydrostatic pressure is exerted on it, balanced by the body's internal forces. Then work is not performed. Dynamic equilibrium is accomplished in the exchange of momentum between the vacuum and body; in the vacuum an inhomogeneity exists (a gravitational field), characterized by the existence of an equilibrium exchange.

With linear and uniform motion, neither the gravitational vacuum nor the moving bodies gain additional momentum. Over sufficiently long intervals of time and space, the following equality is fulfilled (over a short interval it can also not be fulfilled):

$$p_i + p_e = 0, \quad \frac{dp}{dt} = 0,$$

where p_i is the impulse particles of the gravitational vacuum impart to the body, and p_e is the impulse of the body imparted to the gravitational vaccum.

This equality means that if external forces are not exerted on the body, then it either is at rest or it moves without acceleration. The linear and uniform motion which has already originated is not evidenced in any manner.

2. With acceleration of the body's motion under the influence of an external force or under the gravitational influence of bodies on one another, the dynamic equilibrium in the exchange of momentum between the bodies and the gravitational vacuum is disturbed because of the fact that it is restored not instantaneously, but at a rate not greater than the speed of chaotic motion of the particles of the gravitational vacuum.

In the process of an increase in the body's traveling speed, particles of the vacuum are captured by it. The more the body accelerates, the more particles will be captured by it and the greater the increase in the external impulse required in order to change its speed. In this case the energy of external forces results in a change in the mass (energy) of the body:

$$\left(\frac{dp}{dt}\Delta s\right) = \Delta A = \Delta mc^2, \tag{1}$$

where dp/dt is the external force; p is the external impulse; m is the mass of the body; A is the energy of external forces; c is the speed of light; and Δs is the increment in the path.

Equation (1) can be rewritten thus:

$$\frac{dm}{dA} = 1/c^2. \tag{2}$$

If the body moves in the direction of the effect of the external force, then the inertia can be expressed via the derivative of the mass in terms of s :

$$F = m\frac{d^2s}{dt^2} = c^2\frac{dm}{ds}. \tag{3}$$

In this way it is possible to explain the origin of inertia and the increase in mass with a change in the speed of the body. Here the increases in mass, Δm, are maintained in the body even after the cessation of the force's influence in subsequent motion through inertia. Work can be performed on account of the inertial momentum of another body or on account of the momentum of the gravitational vacuum. The first type of interaction is called inertial, and the second gravitational.

Inertial interaction takes place when the momentum of inertial motion of one body is transmitted to another via some type of interaction (e.g., gravitational or electromagnetic). Here one body can lose its mass, and the other acquire the same amount, or they will acquire it in one interval of travel and lose it in another, borrowing it from the vacuum and giving it back to it. Their mass will change as a function of the sign of the energy, in keeping with equation (1). Here the sum of masses will remain unchanged for the entire interval of the path and interaction period.

Gravitational interaction takes place when two or more bodies are present in the vacuum. These bodies will mutually screen movements of the particles of the gravitational vacuum. If they are immobilized, dynamic equilibrium in exchange is established, $dp/dt = 0$. And if not, then dynamic equilibrium is disturbed, the bodies will move toward one another under the effect of force $F = dp/dt$ and work will be performed, $\Delta G = (F\Delta s)$. Furthermore, any work on the part of forces of the gravitational vacuum (field), be it acceleration or inhibition of inertial motion, will result in an increase in the body's mass, since it is performed because the body acquires momentum from the vacuum.

Obviously, acceleration of the body on account of the absorption of momentum from the vacuum will be slighter, the greater its speed relative to the vacuum. A body traveling at the speed of the vacuum's particles, even, cannot accelerate. In keeping with the above, the equation for the increase in mass with gravitational interaction will be as follows:

$$\Delta m = \left| \frac{\Delta G}{c^2} \right| \sqrt{1 - \frac{v^2}{c^2}} \,, \tag{4}$$

where v is the body's traveling speed.

The increase in mass on account of gravitational interaction will equal zero when the work of the forces of the gravitational field equals zero and when the body travels at the speed of light. Since the mass of the body depends on the body's speed relative to the vacuum, in equation (4) speed v should be measured in the same system of reference in which the body's mass is measured.

Thus, the interaction of bodies in the vacuum amounts to the fact that bodies can acquire or impart momentum to the vacuum's particles, or through the vacuum impart their own inertial momentum to another body. In gravitational interaction, bodies always pick up momentum from the vacuum, and, consequently, energy, too. In inertial interaction, momentum and energy can both be picked up from the vacuum and be imparted to it. In the inhibition of inertial motion, the radiation of energy into the vacuum should be observed, and in acceleration, on the other hand, the absorption of it by the body from the vacuum. In this connection, it becomes necessary to extend the laws of conservation to the vacuum. If a body having inertial momentum travels in a vacuum in the presence of other bodies, then its mass will change:

$$\Delta m = \left|\frac{\Delta G}{c^2}\right| \sqrt{1-\frac{v^2}{c^2}} + \frac{\Delta A}{c^2} \tag{5}$$

or

$$c^2 \frac{dm}{dt} = \left|\frac{dG}{dt}\right| \sqrt{1-\frac{v^2}{c^2}} + \frac{dA}{dt}, \tag{6}$$

where A is the work performed on account of the inertial motion of another body or system of bodies, and G is the work on account of the gravitational vacuum.

Equations (5) and (6) are approximate, since the relative influence of the increase in masses has not been taken into account in them.

Let us consider two cases of the interaction of bodies.

The first case: Two spheres, A and B, are traveling along a single straight line passing through their centers. In sphere B there is a through opening, ab, freely admitting the other sphere (fig 1).

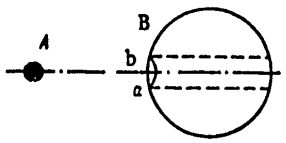

Figure 1. Interaction of Two Bodies Traveling Along a Single Straight Line

Depending on the ratio of speeds and masses, these bodies, having met, can separate forever or can form a system of bodies performing vibrational movements relative to a certain point moving inertially. The velocity of this point will be determined by the result of adding the momenta of these bodies, and the mass of each body will change as a function of whether its inertial motion is accelerated or slowed down. In subsequent vibrational motion relative to the center of inertia, these masses will change. Let us consider the motion of these bodies in a system of reference relating to their center of inertia. At one stage in travel, the bodies, because of gravitational interaction, will travel, under acceleration, toward one another right up to the instant their centers coincide. In the next period their inertial motion in opposite directions, because of gravitational interaction, will be retarded until their speed becomes zero. Then follows attraction of the bodies, and the like.

In the process of this motion, the mass of both bodies will increase on account of gravitational interaction, in keeping with equation (4). In addition to this, in the interval of the path when the motion is accelerated, the direction of acceleration is in line with the direction of movement of the center of inertia, and the body's mass increases, and when the motion is slowed down, the mass is reduced in keeping with equation (1). To the extent that the mass of one body increases, the mass of the other body will be reduced. In body A, on account of inertial and gravitational interaction with body B, the mass will change in keeping with the equation:

$$\frac{\Delta m}{m} = \left| \frac{\Delta W}{c^2} \sqrt{1-\frac{v^2}{c^2}} \right| + \frac{\Delta W}{c^2}, \tag{7}$$

$$\frac{dm}{dt} = \frac{m}{c^2} \left| \frac{dW}{dt} \right| \sqrt{1-\frac{v^2}{c^2}} + \frac{m}{c^2} \frac{dW}{dt}. \tag{8}$$

Here the mass, m, and the speed, v, are determined in the system of reference relating to the system's center of inertia; W is the potential created by body B. Since $\Delta W = (v_0^2/2) \sin (2\pi/T)\Delta t$, then equation (7) will have the form:

$$\frac{\Delta m}{m} = \frac{v_0^2}{2c^2} \left(\left| \sin \frac{2\pi}{T} \Delta t \right| \sqrt{1-\frac{v^2}{c^2}} + \sin \frac{2\pi}{T} \Delta t \right), \tag{9}$$

where t is the period of travel of body A, T is its complete vibration period, and v_0 is the maximum speed of body A.

Thus, if the body were to perform vibrations relative to the center of inertia, then on account of gravitational interaction its mass will increase for the

duration of the entire period (the first term on the right side of equation (9)). On account of inertial interaction (the second term), the mass will increase and be reduced and remain unchanged for the entire period (if the effects of gravitational interaction for the same time are not taken into account).

The second case: Bodies A and B travel so that, as the result of gravitational and inertial interaction, the path of movement of body A is perpendicular to the line of the attractive force of body B. Then because of the fact that the work of the forces of the gravitational field equals zero, the increase in mass will also equal zero. But this motion became possible as the result of a combination of the inertial motion and motion caused by the gravitational attraction of body B. In this case motion takes place in such a way that with the passing of time the conditions for motion under the influence of the force of attraction do not change, as the result of which dynamic equilibrium is established for the momentum gotten and imparted by the body. But with preservation of the constancy of the speed vector in terms of magnitude, its sense changes continuously, since at each point the momentum picked up proves to be directed toward the attracting body. As a result, the effects of the force of gravity boil down to twisting of the path without the performance of work, in keeping with Newton's law, and, consequently, without an increase in mass.

The angle of deflection of the speed vector during period Δt is determined by the equation:

$$\Delta\varphi = \frac{g\Delta t}{v}\sin\alpha,$$

where g is the acceleration of the force of attraction in orbit, and α is the angle between the directions of acceleration of the force of attraction and of velocity v.

The mean angle of deflection of the path will be twofold smaller:

$$\Delta\psi = \frac{g\Delta t}{2v}\sin\alpha. \tag{10}$$

In motion in a circle with an attracting body at its center, the angular velocity will be constant.

As the result of combination of the inertial traveling speed of the center of inertia and the speed of uniform travel along the circle around it, the resultant motion will take place with a linear velocity of variable magnitude, work will be performed, and the mass of the body will change. If body A is much smaller than body B and it travels along a circle around it and the vector of the inertial speed of the center of inertia lies in the plane of

the path of travel of body A, then the increase in the mass of body A can be determined approximately by the equation (fig 2):

$$\frac{\Delta m}{m} \approx \frac{v_1 v_2}{c^2} \sin \omega t,$$

where v_1 is the linear velocity of body A, v_2 is the traveling speed of the center of inertia, $\omega = 2\pi T$, and T is the period of rotation of body A.

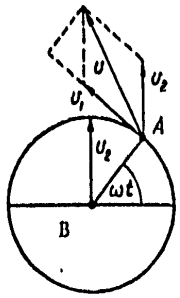

Figure 2. Travel of Body A Along a Circle Around Body B: v_1--linear velocity of body A; v_2--speed of center of inertia; v--resultant speed

When there is an angle β between the plane of the path of travel of body A and the sense of the inertial speed vector, then the relative increase in mass can be determined by the equation:

$$\frac{\Delta m}{m} = \frac{v_2 v_1}{c^2} \cos \beta \sin \omega t. \tag{11}$$

Thus, in this case gravitational interaction results only in twisting of the path, and inertial interaction will be accompanied first by a positive and then by a negative growth in mass. In a complete revolution of body A the growth in its mass will equal zero.

The actual motion of the planets of the solar system takes place in ellipses, which can be considered a combination of the two cases described here. When bodies travel along parabolas and hyperbolas, their masses increase on account of gravitational interaction. But as the result of inertial interaction, in the end result the growth in masses will equal zero.

Thus, the properties described above, of a corpuscular model of gravitation and inertia, are based on the following main assumptions:

1. The particles of a gravitational vacuum have a critically high traveling speed, which cannot be exceeded by the speed of physical interactions and rate of information propagation.

2. In inertial motion dynamic equilibrium is accomplished in the exchange of momentum between bodies and the vacuum.

3. Accelerated motion of a body relative to the vacuum is accompanied by the transfer of momentum from the vacuum to the body and, vice-versa, from the body to the vacuum, and by the transfer of momentum from one body to another.

Furthermore, any work of forces is accompanied by a change in the body's mass. An increase in the body's mass is accompanied by the absorption of momentum from the vacuum, and a reduction in it, on the other hand, by radiation of it into the vacuum. Therefore, for the corpuscular model of gravitation and inertia, the laws of conservation must also cover a gravitational vacuum.

In the corpuscular model there inevitably exists a system of reference relating to the vacuum. Acceleration (increase in mass and absorption of the vacuum's particles) and retardation (reduction in mass and radiation of momentum into the vacuum) are discussed in relation to the vacuum. The very assumption of the existence of a critical speed for physical interactions is an acknowledgement of the fact of this system's existence. It is possible to hypothesize that the existence and travel of the bodies themselves owe themselves to the vacuum, and that when the bodies reach the critical speed the conditions for their existence disappear [4,5]. But the actual motion of bodies is determined in relation to an arbitrarily selected system of reference. Therefore, an increase in mass can be found only in relation to the mass of the state of motion of the body in the system of reference in relation to which the work or increase in momentum are computed. The sign of the increase in mass can be determined from non-inertial effects, such as the change in the rate of inertial rotation, the change in the body's weight, and the like.

Effects of the Corpuscular Model of Gravitation and Inertia

Change in Mass of the Planets Versus Their Gravitational Interaction with the Sun

The planets of the solar system travel in elliptical orbits, being drawn closer to and farther away from the Sun. Here the gravitational field performs work. Regardless of the sign of this work, the mass of the planets and Sun will be increased. For the same reason the mass of the planets will increase when they rotate on their own axes. An estimate of these effects is give in [6], and the main results of these estimates are given in table 1.

In calculating the increase in Earth's mass on account of rotation on its own axis, the increase in its density from the surface to its core is taken into account. For the other planets the density is assumed to be constant.

Table 1.

1) Планета	7) Относительное приращение массы планет за земной год, обусловленное вращением	
	8) вокруг Солнца	9) вокруг собственной оси
2) Земли	$6{,}6 \cdot 10^{-10}$	$2{,}06 \cdot 10^{-10}$
3) Меркурий	$9{,}2 \cdot 10^{-8}$	$0{,}12 \cdot 10^{-10}$
4) Марс	$1{,}3 \cdot 10^{-9}$	$0{,}5 \cdot 10^{-10}$
5) Венера	$0{,}1 \cdot 10^{-10}$	$0{,}2 \cdot 10^{-11}$
6) Юпитер	$0{,}31 \cdot 10^{-10}$	$2{,}8 \cdot 10^{-10}$

Key:

1. Planet
2. Earth
3. Mercury
4. Mars
5. Venus
6. Jupiter
7. Relative increase in mass of planets during terrestrial year caused by rotation
8. Around Sun
9. On own axis

The increase in mass of planets on account of travel around the Sun takes place uniformly, and on account of movement on their own axes it is proportional to the distance from the axis of rotation. The effect of an increase in the mass of Earth must result in secondary effects [6], such as an increase in its dimensions, extension of the period of rotation on its own axis, an increase in the force of gravity on its surface, shortening of the year and an increase in temperature. The effect of an increase in the mass of planets should be evidenced in evolution of their orbits, in particular, in rotation of the perihelion. By an increase (cf. table 3) in the dimensions of Earth it is possible to explain such geological facts as the correspondence in the configurations of coastlines of neighboring continents, the apparent drift of continents, the expansion of oceans, the young age of rocks making up their floor, differences in the structure and composition of the crust of continents and oceans, and the presence of numerous faults.

By the non-uniformity in the increase in mass in the crust it is possible to explain orogenesis and folding, periodic uplifts and subsidence of the ground surface, the oblateness of Earth at its poles, and the reduction in the number of earthquake centers per unit of area from the equator to a pole. The pear-shaped form of the Moon can also be related to a non-uniform increase in mass, because of the fact that it always has one side facing Earth.

Periodic Change in Mass of a Planet from Its Inertial Interaction with the Sun

The planets and Sun travel in ellipses around a certain point moving inertially. As was demonstrated above, this motion, because of inertial

interaction, should result in a periodic change in the mass of planets and the Sun. An increase or decrease in the mass of the planets takes place on account of a corresponding change in the mass of the Sun. For the purpose of simplifying calculations, let us assume that the planets travel not in ellipses, but in circles (cf. fig 2). Then, for an approximate computation of the relative increase in mass it is possible to use equation (11), where v_1 is the linear velocity of a planet when it is traveling around the Sun, v_2 is the inertial velocity of the solar system relative to fixed stars, and β is the angle between the plane of the planet's orbit and the vector of the solar system's inertial velocity.

The real values of v_2 and β are unknown to us. It is known very approximately that the Sun moves at a velocity of 20 km/s toward a point with coordinates of $\alpha = 270°C$, $\beta = 30°$. Taking this into account, we find an amplitude for the relative increase in mass of planets which is somewhat too high, since we have assumed that $\cos \beta = 1$.

Table 2.

1) Планета	2) Период обращения вокруг Солнца в земных годах	3) Амплитуда относительного приращения массы планеты $\frac{\Delta m}{m} \cdot 10^9$	4) Амплитуда относительного изменения массы Солнца под влиянием планеты $\frac{\Delta m}{m} \cdot 10^{14}$	5) Амплитуда изменения периода вращения планет вокруг собственной оси $\Lambda \cdot 10^4$, с
6) Земля	1	6,6	2	5,8—9,6
7) Меркурий	0,24	10,1	0,2	5400—9200
Венера	0,61	8,2	2,2	1700—2850
8) Марс	1,88	5,4	0,2	5—8,2
9) Юпитер 10)	11,86	2,9	277,2	1—1,7
Сатурн 11)	29,5	2,2	63,6	—
Уран 12)	84	1,4	6,4	—
Нептун 13)	164	1,2	6,4	—
Луна * 14)	0,075	0,12—0,56	144—680	—

15) * Движение вокруг Земли.

Key:

1. Planet
2. Period of revolution around Sun in terrestrial years
3. Range of relative increase in mass of planet, $(\Delta m/m) \cdot 10^9$
4. Range of relative change in mass of Sun under influence of a planet, $(\Delta m/m) \cdot 10^{14}$
5. Range of change in period of rotation of planets on their own axes, $\Lambda \cdot 10^4$, s
6. Earth
7. Mercury
8. Venus
9. Mars
10. Jupiter
11. Saturn
12. Uranus
13. Neptune
14. Moon
15. Travel around Earth

In table 2 are given the ranges of relative changes in the mass of planets and the Sun, and also ranges of the change in the period of rotation of planets on their own axes. Since the parameters of the Sun's motion relative to remote stars have been determined unreliably, experimental data on changes in the period of rotation of the planets on their own axes and in the acceleration of the force of gravity can refine them. A periodic change in the mass of planets and the Sun is apparently accompanied by periodic radiation of energy into the vacuum and absorption of it from the vacuum, which in turn can influence the state of matter and processes occurring in the planets and the Sun. The greatest influence on the Sun is exerted by Jupiter, with a period of revolution of 11.86 years. The cyclicity of solar activity, with an 11-year period, can be related to the influence of Jupiter, complicated by the influence of other planets, primarily of Saturn, and then of Venus, Earth, Uranus and Neptune. It is possible to hope that more careful studies of the phenomenon of the variability of solar activity will reveal effects related to the influence of other planets on the Sun. A periodic change in the mass of planets can result in periodic changes in the length of the day, which can be detected experimentally. The so-called seasonal variations in the length of the day observed on Earth are close to those computed. Usually these variations in the length of the day are related to seasonal movements of air masses. This relationship cannot be considered totally substantiated, since seasonal variations in both hemispheres are mutually opposed and the only thing that can be shown is asymmetry of the dry land and sea and the elliptical nature of Earth's orbit, resulting in the fact that Earth over the course of the year draws near to and farther away from the Sun. When it nears the Sun, Earth's rate of rotation must be reduced, and when it draws away from it, increased, as the result of the rising and lowering of air masses.

In our opinion, the major share of seasonal variations is associated with a change in Earth's mass. Movements of air and water masses can only complicate the pattern.

Periodic changes in the mass of planets must be accompanied by a change in the acceleration of gravity at their surface. On Earth the range of these changes can reach $6 \cdot 10^{-6}$ cm/s^2. Therefore, there will be nothing remarkable about the fact that geological phenomena (earthquakes, eruptions of volcanoes) correlate with periods of the year.

Inertial interaction of Earth and the Moon must result in an influence of the Moon on Earth with a rather high range. Therefore, it is possible to hope to discover on Earth the influence of the Moon on the nature of the occurrence of various processes.

Deflection of a Light Beam by the Sun

The motion of a planet around the Sun can be divided in two: One component is motion in a circular orbit without an increase in mass, and the other is motion perpendicular to it with an increase in momentum and mass. The first agrees with Newton's law, and the second exactly differentiates the corpuscular model from Newton's mathematical model. Let us find the numerical relationships

between these effects. For this purpose let us consider the motion of Mercury and Earth. In one second the increase in Mercury's mass equals $\Delta m/Tm = (2.2 \cdot 10^{-8})/(0.76 \cdot 10^{7}) = 2.9 \cdot 10^{-15} s^{-1}$. As was assumed previously, the particles of the gravitational vacuum travel at the speed of light, $3 \cdot 10^{10}$ cm/s. Then the relative increase in momentum--the acceleration--will equal $u = \Delta m/m \cdot c/t = 8.7 \cdot 10^{-5}$ cm/s^2, where t is the length of a year in seconds. Dividing this figure for acceleration by ordinary Newtonian acceleration in Mercury's orbit, we find that $u/g = 2.15 \cdot 10^{-5}$. For Earth the ratio of u/g equals $1.37 \cdot 10^{-6}$. Since both one effect and the other are inversely proportional to the square of the distance, then the total proportionality factor, the gravitational constant in Newton's law, represents well their combined effect. So it will be until we have to deal with low relative velocities for the interacting bodies or with a weak gravitational field.

Let us assume that one of the bodies is light and we will find the bend in its beam when passing near the Sun. Before beginning any computations, let us introduce some assumptions.

1. Light is not accelerated and not retarded in the gravitational field.

2. When the beam travels along a line perpendicular to the direction toward an attracting body, light, as does any other body, bends it path in keeping with Newton's law, i.e., with equation (10).

3. When the beam moves in the direction of the attracting body, it changes its mass and energy as a function of the change in gravitational potential, i.e., in keeping with equation (7), where $v = c$ acquires a momentum of Δmc, directed toward the attracting body. According to this, the motion of the beam can be represented as consisting of motion directed toward the attracting body and motion perpendicular to it. Thus, bending of the beam will consist of ordinary Newtonian, without an increase in mass, and of corpuscular, with an increase in mass.

Let us assume that the beam in traveling from a star to Earth touches the solar disk and that it is bent very slightly; therefore in deriving equations it is possible to disregard it (fig 3). Corpuscular bending of the beam, $\Delta\psi_k$, in segment Δs equals:

$$\Delta\psi_k = \alpha \frac{\Delta m}{m},$$

where α is the angle between the line of the beam and the line to the center of the Sun and $\Delta m/m$ is the relative increase in mass (beam energy) computed by equation (7). Substituting the values of α and $\Delta m/m$ in this equation, we find that:

$$\Delta\psi_k = \frac{ks}{c^2 (R^2 + s^2)^{3/2}} \operatorname{arcctg} \frac{s}{R} \Delta s,$$

where k is the Sun's constant.

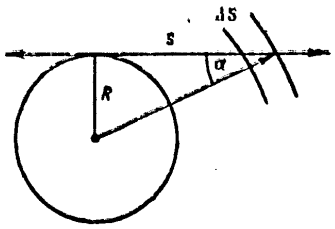

Figure 3. Sketch for Calculating Deflection of a Light Beam by the Sun

The deflection for the beam found, $\Delta\psi_k$, takes place on account of the component of its motion along the line toward the center of the Sun. On account of the component of Newtonian motion along the perpendicular line, the beam is deflected in keeping with equation (10):

$$\Delta\psi_H = \frac{kR\,\Delta s}{2c^2\,(R^2+s^2)^{3/2}}.$$

After integrating, we find:

$$\psi = \psi_k + \psi_H = \frac{k}{c^2 R}(n-1).$$

This equation will be accurate only in the case of slight deflection of the beam. In calculating, the following results were gotten: $\psi_k = 0''51$, $\psi_H = 0''44$, and $\psi = 0''95$. This deflection of the beam was detected by observing the covering of a star by the solar disk during an eclipse. Because of deflection of the beam, the star will be visible still, when the solar disk obscures from view the straight line from the star to the observer, and it will become visible before the solar disk uncovers this line. Therefore, angle ψ must be doubled, i.e., $2\psi = 1''9$.

In table 3 are given the results of calculations and of experimental determinations of certain effects.

Comparison of the calculation and experimental results shows totally satisfactory agreement. The rotation of the perihelion of Mercury according to the calculated data is somewhat less than the experimental. This can be explained by insufficient accuracy of the calculations. The difference in results for the rotation of the perihelion of Earth, of 2.5 percent, is apparently related to inaccuracy of the experimental data, and perhaps to an imprecisely dense model of Earth. Regarding the rotation of the perihelion of Venus the same can be said as about Earth.

Table 3.

Effect	Calculated data	Experimental data	Source of experimental data
Secular increase in period of rotation of Earth on its own axis in one year, seconds	$(7.4 \text{ to } 12.5)\cdot 10^{-5}$	$(10 \text{ to } 15)\cdot 10^{-5}$	[2]
Secular increase in radius of Earth in one year, cm	<0.2	0.6 to 1	[3]
Secular increase in gravity on surface of Earth, cm/s^2	$(2.3 \text{ to } 8.5)\cdot 10^{-7}$	$<1\cdot 10^{-6}$	
Secular reduction in period of revolution of Earth around Sun in one year, seconds	$5.84\cdot 10^{-3}$	$(5.3 \text{ to } 6.7)\cdot 10^{-3}$	[10]
Secular rotation of the perihelion of Mercury in 100 terrestrial years, from arc	42.56	42.6	[8]
Secular rotation of the perihelion of Earth in 100 terrestrial years, from arc	4.02	3.8	[8]
Secular rotation of the perihelion of Venus in 100 terrestrial years, from arc	6.97	8.4	[7]
Range of seasonal variation in the period of rotation of Earth on its own axis, seconds	$(5.8 \text{ to } 9.6)\cdot 10^{-4}$	$10\cdot 10^{-4}$	[1]
Range of seasonal variations in gravity, cm/s^2	6.10^{-6}	-	
Deflection of light beam from star by Sun	1"9	2"	[7]

The satisfactory agreement of the calculated and experimental data for the rotation of the perihelion of Earth while taking into account rotation on

its own axis and the distribution of density within it is a strong argument in favor of the corpuscular model of the gravitational field. Precise determinations of the rotation of perihelia of the planets can give valuable information on the distribution of density within planets, and in certain instances on the period of their rotation. The satisfactory agreement of the calculation and experimental results for the deflection of a light beam from a star by the Sun also testifies to the correctness of the mechanism of gravitational and inertial interaction employed in the corpuscular model.

The secular variation in the period of rotation of Earth on its own axis, besides the growth in mass, depends on Moon-Earth tidal interaction, which results in lengthening of the day. The movement of heavy components toward the core and of light toward the surface, on the other hand, results in shortening of the day. Therefore, it is difficult to expect precise agreement between the calculation and experimental results.

The range of periodic variations in Earth's rate of rotation agrees satisfactorily with the experimental. The discrepancies present can be fully explained by the radial migration of masses in the atmosphere and hyrdosphere, and perhaps also in the substance of Earth. This migration can be correlated with the movement of other planets because of their influence on the activity of processes in the Sun.

The experimental data on the increase in Earth's radius are highly approximate. No less approximate also are the results of calculations characterizing only the upper limit. Periodic secular variations in gravity have been modified several times depending on the model used for the increase in mass. And the experimental data which would make the selection of a model more definite have as yet been insufficiently accurate. Improvement in the accuracy of data on variation in gravity has been hampered not only by insufficient accuracy of the measuring equipment, but also by interference related to relative variations in gravity, which can be explained by relative horizontal and vertical movements of layers of Earth. Reliable experimental data can be gotten only by simultaneous measurements at many uniformly spaced points on Earth. Relative variations in gravity should be much slighter at the poles than at the equator.

As far as variations in the length of the year are concerned (the tropical or Bessel), it can be considered that the calculated and experimental data agree satisfactorily, if the not too high accuracy of the experimental data is taken into account.

In conclusion, let us summarize the above.

1. The corpuscular model of gravitation and inertia satisfactorily explains the existence of forces of gravitational interaction and forces of inertia, and physically interprets the inferences of the theory of relativity.

2. This model demonstrates that our solar system, as is the entire universe, is evolving, and explains certain geological and geophysical phenomena.

3. The experimental data confirm the existence in macrosystems of the effect of an increase in mass with gravitational interaction and of a change in mass with inertial. An increase in mass will evidently also take place in a variable gravitational field (gravitational and inertial induction of mass).

4. It is a very good idea to set up experiments with rotating bodies and artificial satellites for the purpose of confirming the corpuscular model of gravitation and inertia. They should be set up in order to explain the mechanism for an increase in mass in a gravitational field, i.e., in addition to weighing, a precise physical chemical analysis should be made of the models before the experiment and after it.

5. It is necessary also to improve the accuracy of determining the rate of rotation of Earth and the other planets on their own axes and of their revolution around the Sun, the rates of the rotation of perihelia and their orbits, and the characteristics of solar activity, and to arrange for research on geological, geophysical and biological phenomena caused by the evolution of the solar system.

Bibliography

1. Bakulin, P.I., Konopovich, E.V. and Moroz, V.I. "Kurs obshchey astronomii" [Course in General Astronomy], Moscow, Nauka, 1974, 133 pages with illustrations.

2. Belotserkovskiy, D.Yu. "Results of Recent Investigations of the Rate of Earth's Rotation" in "Vrashcheniye i prilivnyye deformatsii Zemli" [Rotation and Tidal Deformations of Earth], Kiev, Naukova Dumka, 1970, pp 52-56.

3. Bott, M. "Vnutrenneye stroyeniye Zemli" [Internal Structure of Earth], Moscow, Mir, 1974, 324 pages with illus.

4. Veselov, K.Ye. "Variation in Gravity Over Time and the Corpuscular Hypothesis on Gravity," PRIKLADNAYA GEOFIZIKA, No 73, Moscow, Nedra, 1974, pp 143-150 with illus.

5. Veselov, K.Ye. "Some Geological and Geophysical Consequences of the Corpuscular Model of a Gravitational Field," PRIKLADNAYA GEOFIZIKA, No 80, Moscow, Nedra, 1975, pp 200-212 with illus.

6. Veselov, K.Ye. "Geophysical Effects of the Corpuscular Model of a Gravitational Field," PRIKLADNAYA GEOFIZIKA, No 84, Moscow, Nedra, 1976, pp 121-133 with illus.

7. Ivanenko, D. "Fundamental Problems in Gravitation" in "Noveyshiye problemy gravitatsii" [Recent Problems in Gravitation], Moscow, IL, 1961, pp 33-34.

8. Landau, L.D. and Lifshits, Ye.M. "Teoriya polya" [Field Theory], Moscow, Fizmatgiz, 1960, 349 pages with illus.

9. Ryabov, Yu.A. "Dvizheniye nebesnykh tel" [Motion of Heavenly Bodies], Moscow, Fizmatgiz, 1962, 213 pages with illus.

10. Duboshin, G.N., ed. "Spravochnoye rukovodstvo po nebesnoy mekhanike i astrodinamike" [Manual on Celestial Mechanics and Astrodynamics], Moscow, Nauka, 1971, 119 pages with illus.

8831
CSO: 8144/0854A

GEOPHYSICS, ASTRONOMY AND SPACE

UDC 550.831.23

METHODS OF ESTIMATING THE ACCURACY, NETWORK DENSITY AND ISOANOMALY CROSS SECTION OF A GRAVIMETRIC SURVEY

Moscow PRIKLADNAYA GEOFIZIKA in Russian No 87, 1977 pp 111-121

[Article by B.P. Surovtsev]

[Text] At the present time there are several different methods of determining the parameters of a gravimetric survey. Each of these is based on certain apriori assumptions regarding the properties of the useful signal and noise and in them are utilized different criteria for detecting and separating the signal, and different software is used.

Let us compare several methods of calculation as applies to the problem of scanning mildly sloping platform structures. We know that mildly sloping structures create gravity anomalies with an intensity of 0.1 mgal and minimum dimensions of 1 to 2 km [4,8]. These data form the basis of all subsequent calculations.

According to "Technical Instructions for Gravitational Prospecting Operations," a gravity anomaly is considered reliably identified if it is intersected by a minimum of two sections and is confirmed by a minimum of three points. Furthermore, the root-mean-square measurement error must not be greater than 0.3 times the intensity of the anomaly [2]. As applies to prospecting of mildly sloping structures, this means that required are an observation network density of not less than 0.5 X 1 km and a survey error of 0,03 to 0.05 mgal. The survey scale corresponding to these parameters equals 1:25,000, and the isoanomaly cross section, 0.25 mgal. But we have no knowledge of the alteration of quantitative relationships between the network density and the accuracy of the survey [2]. Below are presented methods which to one degree or another solve these problems.

In 1958 B.V. Kotlyarevskiy suggested that a determination be made of the parameters of the small-scale surveys widespread at the time by means of the method of relative errors [3]. Its essence consisted in determining survey parameters on the basis of selecting specific relative errors in the detection of gravity anomalies and in determining the growth in these anomalies within the limits of the chart's cross section. Apriori assignment of errors made

it possible automatically to find the network density, survey accuracy and scale and isoanomaly cross section required in this case.

Let us discuss this method as applies to the problem of prospecting mildly sloping structures. We will assume that the mean distance between observation points, a , expressed in fractions of ℓ , half of the linear dimensions of the effective anomaly, varies within the range of $0.1 \leq a/\ell \leq 1.5$, and the survey error, σ , varies from 0.02 to 0.15 mgal.

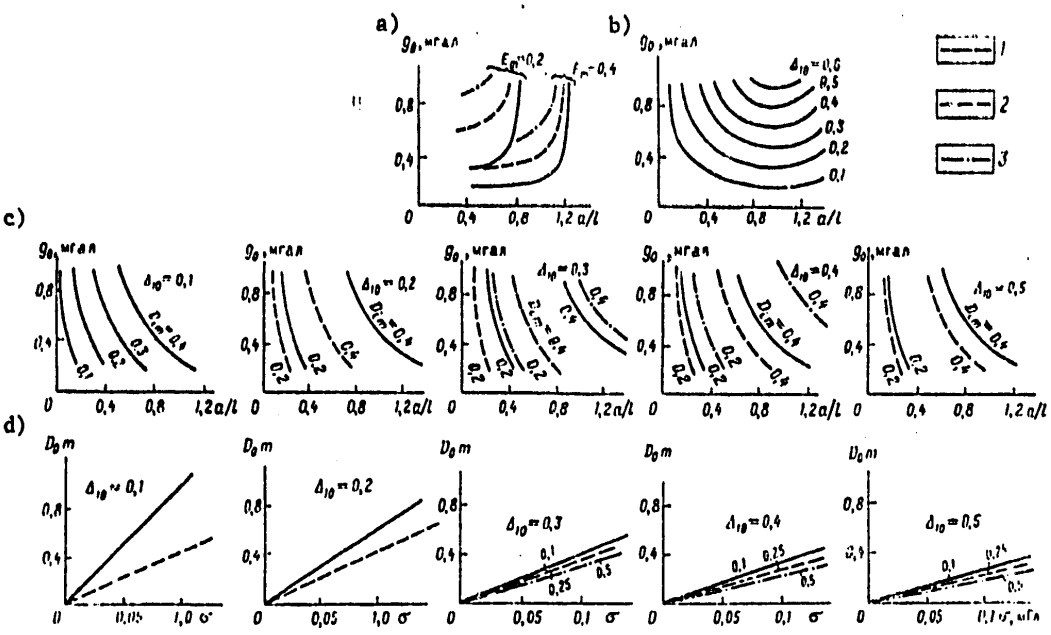

Figure 1. Curves for Calculating Survey Parameters by Using the Method of Relative Errors E_m and D_m :
a--curves for equal values of relative error E_m : 1--σ = $\pm$ 0.05 mgal; 2--σ = $\pm$ 0.10 mgal; 3--σ = $\pm$ 0.15 mgal;
b--curves for equal increments of A_{10} (g_0 is the maximum prospecting anomaly and a/ℓ is the interval between observation points in fractions of half the distance between adjacent extremes); c--curves for equal values of relative error D_{1m} :

[Caption continued on following page]

1--P = 0.1 mgal; 2--P = 0.25 mgal; 3--P = 0.5 mgal; d--curves for relative error D_{ot} : 1--P = 0.10 mgal; 2--P = 0.25 mgal; 3--P = 0.50 mgal

In fig 1a are given curves by means of which, for fixed values of the relative error in identifying an anomaly, E_m (0.2 and 0.4), with a selected survey accuracy, σ , (0.05, 0.10 and 0.15 mgal), it is possible to select the relative network density, a/ℓ , for the purpose of identifying the effective anomaly with a predetermined maximum intensity, g_0 . From consideration of these curves it can be concluded that in identifying an anomaly, g_0 , with an error of σ , an increase in the relative network density, a/ℓ , corresponds to a reduction in relative error E_m , and, on the other hand, in identification of an anomaly, g_0 , a simultaneous reduction in the network density ($a/\ell \to \infty$) and increase in accuracy of the survey ($\sigma \to 0$) makes it possible to maintain relative error E_m constant, and the same is true with a simultaneous increase in network density ($a/\ell \to 0$) and reduction in accuracy ($\sigma \to \infty$). With an assigned network density and survey accuracy, a smaller relative error, E_m , corresponds to a greater intensity, g_0 , and linear dimensions, 2ℓ , and vice-versa. These dependences broaden the opportunities for selecting the network density and survey accuracy. Furthermore, depending on specific conditions, it is possible to modify the parameter by means of which in the specific instance it is simpler to reach the required relative error, E_m .

In determining the isoanomaly cross section and the survey scale corresponding to it, in the method is employed an auxiliary function for the increase in gravity, Δ_{10} , between neighboring observation points within the limits of the effective anomaly. In fig 1b are shown curves for equal values of Δ_{10} versus the maximum intensity of the anomaly, g_0 , and the relative network density, a/ℓ . The values selected for Δ_{10} serve as the basis for plotting auxiliary curves for components D_{im} and D_{0m} of the total relative error in determining the increase in anomalies ($D_m = \pm \sqrt{D_{im}^2 + D_{0m}^2}$) within the limits of the charts' cross section.

In fig 1c are given series of curves for equal values of component D_{im} as a function of the relative network density, maximum intensity of the anomaly and the increase, Δ_{10} , between neighboring points and isoanomaly cross section, P . All series have been plotted for three fixed cross sections (P = 0.1, 0.25 and 0.5 mgal) and corresponding survey scales, 1:10,000, 1:25,000 and 1:50,000. The values of D_{0m} are determined from the curves in fig 1d.

Practical determination of the required cross section, P , reduces to the following: a) A determination is made of the increment function, Δ_{10} , with an assigned relative network density and maximum intensity of the anomaly. b) A selection is made, by means of the nearest fixed value of Δ_{10} , of the required curves for the components of the relative error, D_m . With an assigned error of $D_m = \pm \sqrt{D_{im}^2 + D_{0m}^2}$, from the curves selected a determination is made of the required isoanomaly cross section, P , and, consequently, of the survey scale, too.

Thus, the cross section and survey scale determine the degree of certainty in finding the increment in gravity within the limits of the effective anomaly, i.e., the degree of reliability in determining the regularities in the anomaly's structure. By varying the degree of reliability within reasonable limits, it is possible to alter the isoanomaly cross section and survey scale. On the whole, the method of relative errors opens up extensive opportunities for varying survey parameters. It makes it possible, taking into account the equipment available and local conditions, to select those parameters which ensure the required relative errors, E_m and D_m, with the smallest loss of materials, and, consequently, with the greatest savings. Among the method's disadvantages must be placed the absence of procedures for determining survey parameters in the case of detection and isolation of an anomaly commensurate with the noise ($E_m \geq 0.5$ and $D_m \geq 1$). In addition, all computations are made within the limits of an individually taken profile.

Let us now discuss three other methods which suggest determination of the network density and survey accuracy on the basis of a statistical approach to solving the problem. They are based on the following apriori assumptions regarding the properties of effective anomalies and noise: a) Gravity anomalies and random observation errors are regarded as steady-state random functions satisfying the condition of ergodicity. b) These functions are isotropic in the statistical respect, i.e., the second correlation factor is constant for the entire territory considered. c) Random observation errors are distributed according to a normal law so that their first correlation factor equals zero, and their second correlation factor is not higher than 1.5 times the distance between observation points.

In 1964 I.D. Savinskiy suggested a method for finding the optimum observation network density while estimating the certainty of detection of the subject of the search [4]. The essence of this method consisted in estimating the probability, P_n, of a sub-cross-section by the points of an orthogonal observation network for objects of elliptical shape. The author put together tables and, on their basis, auxiliary nomograms for estimating P_n, in which taking part as parameters are fixed values of the ellipse's contraction coefficient and of the distance between profiles, expressed in fractions of a unit of length of the object (major axis of the ellipse). By assigning a specific probability of detection of the object, on the basis of its dimensions, by means of the tables (nomograms) is automatically found the required observation network density. A positive advantage of this method is the simplicity of estimation, based on the criterion of certainty of detection. Furthermore, in each specific instance the optimum certainty is determined by taking into account the economic indicators for the cost of the job. At the same time it should be stressed that the capabilities of this method are limited, since it does not consider such an important characteristic as the survey's accuracy and its relationship to the strength of the useful signal. In view of this, the application of this method is not possible in gravitational prospecting, in particular.

In 1967 K.V. Gladkiy suggested determining the interval, L, between observation points, which enables the achievement of equality in the r.m.s. errors

at observation points, $\bar{\sigma}$, and in the interval between them, $\bar{\varepsilon}$. On the basis of this condition, for a point situated in the interval of L/2, he derived an equation for the relationship between the mean statistical function of the square of the effective anomaly, B(0) , the network density autocorrelation function, B(l) , and the r.m.s. error at observation points, $\bar{\sigma}$ [1]:

$$\bar{\varepsilon}^2 = \bar{\sigma}^2 = 3B(0) + B(l) - 4B(l/2). \tag{1}$$

We made a study of this equation as applied to the problem of prospecting mildly sloping structures. For this purpose, the gravitational effect of a mildly sloping structure is approximated by the influence of a contact surface with excess density, $\Delta\rho$, at a boundary located at a mean depth of $\bar{H}$, and having a mean statistical amplitude of $\bar{Z}$ and correlation radius of R_z . Taking into account the apriori assumptions discussed above, regarding the properties of anomalies and random noise, the following problem has been formulated: Estimate the maximum interval, L , between observation points making it possible to achieve at point L/2 an r.m.s. error, ε , in the value of the anomaly prospected, interpolated linearly, equal to the r.m.s survey error, $\bar{\sigma}$.

Let us substitute in equation (1) expressions, B(0) , for the contact surface and network density autocorrelation function, $B(L) = B(0) \exp(-L^2/r^2)$ [5]. After transforms, equation (1) is written in the form:

$$X^4 - 4X - A = 0, \tag{2}$$

where $X = \exp[-(LK/2R_z)^2]$ and K is a certain auxiliary function:

$$K^2 = 1 - \frac{2\bar{H}}{R_z}\sqrt{\pi}\exp(2\bar{H}/R_z)^2[1 - \Phi(2\bar{H}/R_z)];$$

$$A = \bar{\sigma}^2/\bar{g}_0^2 K^2 - 3; \quad g_0 = 2\pi f \Delta\rho \bar{Z}.$$

Having solved this equation, unknown interval L can be found from the equation:

$$L^2 = -4R_z^2/K^2 \ln X. \tag{3}$$

The domain for determining X in equation (2) depends on the range of variation of the parameters of the contact surface characterizing the mildly sloping structure ($\bar{H}$, $\bar{Z}$, R_z, $\Delta\rho$) and survey errors, $\bar{\sigma}$. In fig 2 are shown curves for auxiliary functions K^2 and g_0 , which are determined from assigned values for $\bar{H}$, $\bar{Z}$, R_z and $\Delta\rho$.

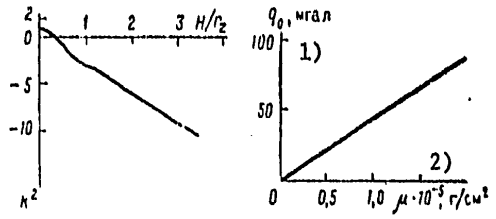

Figure 2. Curves for Estimating Coefficients K^2 and g_0 in the Method of Equating Errors $\bar{\sigma}$ and $\bar{\varepsilon}$

Key:
1. mgal
2. g/cm^2

The advantage of this method is the ability to determine an interval between observation points which ensures equality between errors at observation points and in the interval between them. Among its disadvantages must be listed the limitations imposed by the apriori assumptions regarding the properties of anomalies and noise, the factor of establishing an interval, L , for an individual profile, and the need to solve a quadratic equation.

In 1967 A.A. Nikitin, in discussing questions relating to the detection of slight geophysical anomalies against a background of random noise, touched upon the problem of estimating the observation network density and the accuracy of geophysical surveys [4]. Based on the hypothesis that errors in detection of the useful signal involving a signal gap or the detection of a false signal are equally probable, he suggested a relatively simple equation making it possible to estimate the certainty of detecting a determined anomaly against a background of random noise, in terms of area.

Let us consider A.A. Nikitin's equation in somewhat modified form, characterizing the certainty of detection of a determined anomaly against a background of correlated noise, σ^* , with a delta autocorrelation function, $R = \pm \sqrt{R_x^2+R_y^2}$. For N profiles ($1 \leq i \leq N$) and M points within the limits of each profile ($1 \leq j \leq M$) intersecting the prospected anomaly, we have:

$$\gamma = \Phi\left(\frac{\sqrt{\rho_1+\rho_2+\ldots+\rho_N}}{2}\right), \tag{4}$$

where $\Phi = 2/\sqrt{2\pi}\int_0^t \exp(-t^2/2)dt$ is the probability integral.

Taking part in equation (4) are functions, ρ_i , for the ratio of the energy of the prospected anomaly to the energy of the correlated noise for the i-th profile:

$$\rho_l = \frac{\sum_{j=1}^{M} g^2(x_{lj})}{\bar{\sigma}^{*2}} = \frac{\bar{g}^2 M_l}{\bar{\sigma}^2 R}, \tag{5}$$

where $\bar{g}$ is the mean statistical intensity of the prospected anomaly, $\bar{\sigma}$ is the mean statistical intensity of the random non-correlated noise, and R is the delta autocorrelation function for the noise.

It follows from equations (4) and (5) that the certainty, γ, is directly proportional to the mean statistical strength of the effective anomaly, g, and to the square root of the number of observation points within the limits of this anomaly, and is inversely proportional to the mean statistical strength of the random non-correlated noise, σ, and the square root of the autocorrelation radius of the correlated noise, R.

Equation (4), taking (5) into account, can be rewritten in the form:

$$\bar{g}/\bar{\sigma} = 2\Phi^{-1}(\gamma) \Big/ \sqrt{\sum_{i=1}^{N} M_l / R}, \tag{6}$$

where $\Phi^{-1}(\gamma)$ is a function which is the inverse of the probability integral.

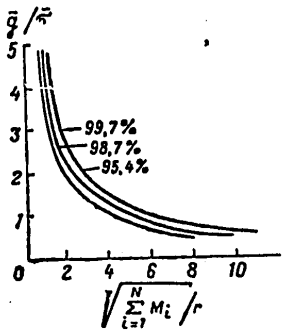

Figure 3. Curves for Estimating Network Density and Survey Accuracy in A.A. Nikitin's Method

In fig 3 are shown curves for the dependence of $\bar{g}/\bar{\sigma}$ on $\sqrt{\sum_{i=1}^{N} M_i/R}$ for three fixed values of the certainty, γ, of detecting an anomaly. It can be concluded from studying them that a different degree of certainty in detecting the anomaly matches up with one and the same observation network density with a different degree of accuracy. Similarly, a different degree of certainty in detection matches up with a different network density with the same degree of accuracy. With an increase in the number of observation points within the limits of the prospected anomaly the certainty of its detection increases. With an increase in the autocorrelation radius of the noise, this certainty diminishes.

This method can be employed with success in detecting slight anomalies, equal to and slighter than the strength of the noise, and not only random non-correlated, but also correlated. Among possible disadvantages of this method should be listed the requirements imposed in the apriori assumptions regarding the properties of anomalies and noise, and also the condition of equal probability of errors of the first and second kind.

All five methods discussed, for determining the parameters of a gravimetric survey, employ the common principle of certainty in the detection of the useful signal against the background of random non-correlated noise. This certainty of the existence of a useful signal is a function of the accuracy and network density of the gravimetric survey.

Let us proceed now to a comparative analysis of the certainty of signal detection in the different methods.

Of course, the specifications of "Technical Instructions for Gravitational Prospecting Operations" are fairly categorical: The signal-to-noise ratio within the limits of the effective anomaly should be not less than three ($s \geq 3$). Then the certainty of detecting the effective anomaly is practically equal to unity ($\Phi(3) = 99.7$ percent). Undoubtedly, detection of the effect of a mildly sloping structure with this certainty practically excludes the possibility of missing it. But in the case of low strength of the effect this imposes quite strict requirements on the accuracy of the survey. In particular, the employment of standard gravimeters ensuring a measurement error of 0.05 to 0.06 mgal can become simply impossible. And this, in turn, can restrain the introduction of gravitational prospecting in the practice of prospecting work. In addition, the instructions do not give an answer to the question of the required observation network density and of the possibility of varying it in relation to the accuracy of the survey. Of course, in practice an attempt is always made to make more than three observations per profile within the limits of an anomaly. But in each specific instance this number is determined arbitrarily.

In V.V. Kotlyarevskiy's method of relative errors, evidently for the first time in domestic practice precise relationships were established between the certainty of detecting anomalies and the accuracy and observation network density required for this. Typically, the relative error itself, $E_m = \sigma/g_m$,

is a value representing the inverse of the effective-signal-to-noise ratio introduced by the instructions ($s = 1/E_m$). Furthermore, unlike the instructions, here this value is not a fixed one. It can vary, being bound only at the lower limit ($s \geq 2$). The assignment of E_m automatically determines the required accuracy and observation network density. Furthermore, the certainty of detecting the anomaly is defined as $\Phi = \Phi(1/E_m)$. In addition, this method assumes that it is possible to vary the parameters of accuracy and observation network density while maintaining the required certainty of detection. On the whole this method broadens the capabilities of gravitational prospecting in formulating different problems.

Of all the methods enumerated above, the most effective, evidently, is A.A. Nikitin's method. This is explained by the following reasons. First, here is most simply expressed the relationship between survey parameters and the certainty of signal detection. Unlike other methods, it can be used for detecting anomalies whose intensity is equal to the strength of the noise and is slighter. This method is the only one in which estimates are made with reference to area and in which the case of correlated noise is considered. Survey parameters are determined here on the basis of an apriori assigned certainty of detecting the subject of the search or of prospecting. With assigned certainty, it is possible to vary both the network density and the observation accuracy. All this makes it possible to recommend this method as the basic one in estimating survey parameters, in particular, in prospecting mildly sloping structures.

Let us now discuss the certainty of signal separation against a background of random non-correlated noise. Generally, this certainty is determined by the accuracy and network density of the survey, the ratio of the useful signal and noise strength, and the law for variation of the strength of the useful signal, and, as a consequence of all this, by the isoanomaly cross section and the survey scale. Formally, both in "Technical Instructions for Gravitational Prospecting Operations" and in B.V. Kotlyarevskiy's method, the certainty is assigned by selecting the isoanomaly cross section. In the instructions this problem is solved on the basis of the principle that the cross section must equal triple the measurement error.

Furthermore, a necessary condition for outlining an anomaly is the presence within its limits of not less than three points obtained on independent trips. As far as the scale of the survey is concerned, it is determined on the basis of its formal relationship to the isoanomaly cross section chosen. The condition imposed on selection of the cross section assumes a degree of certainty in outlining anomalies with isolines which is practically equal to unity ($\Phi(3) = 99.7$ percent). But this concerns only anomalies which are two times greater in strength than the measurement errors. Of course, this method cannot be employed for the purpose of outlining anomalies equal to and slighter than the noise. In other words, these anomalies will be omitted, since they will not be outlined.

The employment of B.V. Kotlyarevskiy's method makes it possible in selecting the cross section to operate with the set of parameters of the anomaly to be

isolated. The selection of the cross section itself here depends on the apriori assigned certainty with which we wish to isolate the anomaly in question, $\Phi = \Phi(1/D_m)$. And this certainty, in turn, depends on the selected network density, the accuracy of the survey and the signal-to-noise ratio (the law of variation of the strength of the useful signal is assigned apriori in this method). This has a direct relationship to the problem of isolating low-strength anomalies. Actually, this method establishes the required quantitative relationships between the certainty of isolating the effective anomaly, survey parameters and the isoanomaly cross section (survey scale), for the case when the intensity of the effective anomaly is commensurate with the observation error, $\Phi(1/D_m) = \Phi(1)$.

The comparative analysis of methods made here can be conducive to improving the geological and economic effectiveness of gravitational prospecting.
In conclusion, let us illustrate the capabilities of these methods with a specific example. We assume that the subject for prospecting is a mildly sloping structure with the following parameters:

Number of gravitationally active boundaries	1
Excess density within limits of gravitationally active boundary, $\Delta\rho$, in g/cm^3	0.2
Mean bed depth of gravitationally active boundary, $\overline{H}$, in km	1
Axisymmetric autocorrelation radius of boundary, R_z , in km	2
Mean statistical amplitude of structure, $\overline{Z}$, in km	0.1
Linear dimensions of anomaly of structure, 2ℓ	4
Mean statistical intensity of effective anomaly, $\overline{g}$, mgal	0.2
Maximum intensity, g_0 , mgal	0.3
Ratio of autocorrelation radius of noise to interval between neighboring survey points	1.5

1) Параметр	2) Методы						
	3) приведенный в технической инструкции (по профилю)	4) относительных погрешностей Б. В. Котляревского (по профилю)		5) равенства погрешностей Г. Е. К. В. Гладкого (по профилю)	6) основанный на теории оптимального приема А. А. Никитина (по площади)		
7) Погрешность измерения, мгал	0,07	0,05	0,10	0,05	0,05	0,10	0,15
8) Густота сети, км	1,5	1,5	2,2	—	2,94 × × 2,94	—	—
9) Масштаб съемки, мгал	1 : 25 000	1 : 25 000	1 : 10000	—		—	—
10) Сечение p	0,25	0,25	0,10	—	—	—	—
11) Достоверность выделения полезной аномалии:							
γ_1	99,73	99,99	95,45	100	—	—	—
γ_2	99,73	98,02	79,05	—	—	—	—

[Key on following page]

Key:

1. Parameter
2. Methods
3. Given in technical instructions, (by profile)
4. B.V. Kotlyarevskiy's method of relative errors (by profile)
5. K.V. Gladkiy's method of equating errors σ and ε (by profile)
6. Based on A.A. Nikitin's theory of optimum reception (by area)
7. Measurement error, mgal
8. Network density, km
9. Survey scale, mgal
10. Cross section, p
11. Certainty of isolating effective anomaly

In the table are given the results of estimates by each method, with an indication of the certainty of detecting, γ_1, and isolating, γ_2, the effective anomaly.

Bibliography

1. Gladkiy, K.V. "Gravirazvedka i magnitorazvedka" [Gravitational and Magnetic Prospecting], Moscow, Nedra, 1967, 318 pages with illustrations.

2. "Instruktsiya po provedeniyu gravimetricheskikh rabot" [Instructions on Carrying Out Gravimetric Work], Moscow, Nedra, 197[illegible] 46 pages with illus.

3. Kotlyarevskiy, B.V. "Estimating the Accuracy of a Gravimetric Survey and Selection of an Intelligent Observation Network and Gravity Isoanomaly Cross Section," PRIKLADNAYA GEOFIZIKA, No 20, Moscow, Nedra, 1958, pp 34-62 with illus.

4. Nemtsov, L.D. "Vysokotochnaya gravirazvedka" [High-Current Gravitational Prospecting], Moscow, Nedra, 1967, 230 pages with illus.

5. Nikitin, A.A. "Statistical Detection of Slight Geophysical Anomalies Against a Background of Random Noise" in "Avtoreferat diss. na soisk. uch. step. kand. tekh. nauk" [Author's Abstract of Dissertation for the Academic Degree of Candidate in Technical Sciences], Moscow, MGRI, 1967, 115 pages with illus.

6. Savinskiy, I.D. "Tablitsy veroyatnostey podsecheniya ellipticheskikh ob"yektov pryamougol'noy set'yu nablyudeniy" [Tables of Probability of a Sub-Cross-Section for Elliptical Objects with an Orthogonal Observation Network], Moscow, Nedra, 1964, 36 pages with illus.

7. Serkerov, S.A. "Investigation of Optimal Transformations of Gravitational and Magnetic Anomalies" in "Avtoreferat diss. na soisk. uch. step. kand. tekh. nauk," Moscow, MINKhiGP, 1965, 136 pages with illus.

8. Surovtsev, B.P. "High-Current Gravitational Prospecting in Scanning and Prospecting Mildly Sloping Structures in the Central Regions of the Russian Platform," PRIKLADNAYA GEOFIZIKA, No 65, Moscow, Nedra, 1972, pp 151-163 with illus.

8831
CSO: 8144/0854A

PUBLICATIONS

LIST OF SOVIET ARTICLES DEALING WITH COMPOSITE MATERIALS

Moscow GOSUDARSTVENNYY KOMITET SOVETA MINISTROV SSSR PO NAUKE I TEKHNIKE. AKADEMIYA NAUK SSSR. SIGNAL'NAYA INFORMATSIYA. KOMPOZITSIONNYYE MATERIALY, In Russian Vol 3, No 24, 1978 pp 3-5

[Following is a listing of the Soviet entries from SIGNAL'NAYA INFORMATSIYA. KOMPOSITSIONNYYE MATERIALY (SIGNAL INFORMATION. COMPOSITE MATERIALS), a bibliographic publication of VINITI. This listing is from Vol 3, No 24, 1978]

[Excerpts]

1. Technology of Fusing Graphite Articles Sealed With Thermal Diffusion Substances. Goryainova, A. V., Lonchuk, L. L., Tatarinova, L. V. "Khim. i neft. mashinostroyeniye", 1978, No. 10, 27.

4. Patent. Method of Manufacture of Bimetallic Tubular Components By Pressure Welding With Heat. Saprygin, V. D., Karakozov, E. S., Bereznikov, Yu. I., Gusev. Yu. V., Il'yevskiy, I. I., Aleksandrov, Yu. G., Kazhokhin, A. B., Vusikov, B. A., Smolin, A. I., Dmitriyev, B. P. [Mosk. vech. metallurg. in-t]. USSR Author's Certificate, (V 23 K 19/00), No 610638, Announced 2.06.75, No 2140671, Published 23.05.78.

5. Patent. Method of Welding High-Alloy Steels. Denisov, B. S., Platonov, V. M., Volkov, A. I., Meylakh, A. I. USSR Author's Certificate, (V 23 K 9/02), No 585927, Announced 25.07.75, No 2159800, Published 1.02.78.

6. Methodology for Studying the Design Strength of Laminar and Anisotropic Materials Based on High-Strength Aluminum Alloys. Rudnitskiy, Ye. N., Miklyayev, P. G., Kudryashov, V. G. "Tekhnol. legk. splavov", 1978, No. 8, 70-73.

14. Internal Oxidation When Heating the Bimetal Silver + Copper. Masterov, V. A., Pozdnyakov, V. M. "Nauch. tr. Gos. n.-i proyekt. in-ta splavov i obrab. tsvet. met.", 1978, No. 58, 28-32.

18. Evaluation and Analysis of Sensitivity of Monitoring the Monoenergetic Electrons of Composite Materials With A Fluctuating Content. Rudenko, V. N., Yunda, N. T. "Defektoskopiya", 1978, No. 9, 72-82.

21. Study of the Corrosion Resistance of Plastic-Clad Metal in Food Industry Environments. Istratov, I. F., Britan, I. M., Nifan'teva, L. V., Dekhtyarenko, N. G., Klyachko, Yu. A. "Korroziya i zashchita met. (Kaliningrad)", 1978, No. 4, 25-31.

24. Contact-Extrusion Welding of Reinforced Materials Based on Low-Density Polyethelyne. Solov'yev, V. P. "Svarochnoye pr-vo", 1978, No. 9, 39-42.

40. Influence of Alloying Nickel With V-Metals On Wetting of Graphite. Kashin, O. A., Dudarev, Ye. F., Borisov, M. D. "Sovmestimost' i adgezion. vzaimodeystviye rasplavov s metallami". Kiev, 1978, 66-69.

7869
CSO: 1870

END